



**NTNU – Trondheim**  
Norwegian University of  
Science and Technology

# Modelling and Optimization of a GTL Plant

**Kristoffer Moen**

Chemical Engineering and Biotechnology

Submission date: June 2014

Supervisor: Magne Hillestad, IKP

Norwegian University of Science and Technology  
Department of Chemical Engineering



## Abstract

A gas-to-liquid process converts gaseous carbon feedstock into more valuable products. Recent technological improvements have led to an increased interest in this production method.[1] This master's thesis has evaluated three different gas-to-liquid configurations to determine which design favors production of longer hydrocarbon chains (wax). All of the configurations were simulated with the AspenTech process simulator HYSYS V8.0, where kinetics from Todic et al. [2] describe the Fischer-Tropsch product distribution. Only one pass through the reactor could be simulated because of the HYSYS implementation limitation, where  $C_1$ - $C_{15}$  alkanes and  $C_2$ - $C_{15}$  alkenes were included as products. Utilization of tail gas from the hydrogen plant resulted in a synthesis gas with a lower  $H_2/CO$  ratio. Larger amounts of longer chains were detected and methane production was less favorable when this synthesis gas was processed in the Fischer-Tropsch synthesis. Configuration 2, where both water and products were separated between three smaller reactors, gave the highest carbon and energy efficiency, namely 31 and 13 %.



## Sammendrag

En gass-til-væske prosess omdanner et karbonholdig råstoff til mer verdifulle produkter. På grunn av nye teknologiske fremskritt har interessen for slike prosesser økt de siste årene.[1] Denne masteroppgaven har evaluert tre forskjellige gass-til-væske konfigurasjoner for å finne et design som favoriserer produksjonen av lengre hydrokarbonkjeder (wax). Alle konfigurasjonene var simulert i AspenTech prosess simulator HYSYS V8.0 der kinetikk modellen av Todici et al.[2] beskrev produktfordelingen i Fischer-Tropsch prosessen. Implementeringsbegrensinger i HYSYS gjorde det kun mulig å inkludere  $C_1$ - $C_{15}$  alkaner og  $C_2$ - $C_{15}$  alkener som produkter. Resirkulering av uomsatte reaktanter var heller ikke gjennomførbart. Utnyttelse av en  $CO_2$  innholdsrik gasstrøm fra hydrogenproduksjonen gjorde det mulig å produsere en syntesegass med lavere  $H_2/CO$  forhold. Det ble observert en produksjonsøkning av lengre hydrokarbonkjeder når denne gassen ble prosessert i Fischer-Tropsch prosessen. Mindre favorisering av metan produksjonen var også en klar respons. I konfigurasjon 2 var både vann og produktene fjernet mellom tre mindre reaktorer. Det var denne konfigurasjonen som ga høyest karbon og energieffektivitet, 31 og 13 %.



## Preface

This master's thesis was written at the Department of Chemical Engineering (NTNU) in the spring of 2014. The overall theme of the project was the gas-to-liquid process, where the Fischer Tropsch synthesis has been the main focus.

Supervisor of the project was prof. Magne Hillestad, and I will use this opportunity to thank him for guidance and good advice during this project.

I would like to thank my good friend and room-mate, Fredrik Nordmoen. You took time to discuss and help me through frustrating programming issues which i'm very thankful for. One other person I want to mention is PhD student Mohammed Ostadi. His enthusiasm, determination and laughs have been a true blessing through this project. At last I would thank my best friend in Trondheim, Christer Haugland. You have always been interested in my project and all of our discussions have made a large impact on the final product.

### **Declaration of compliance**

I declare that this is an independent work according to the exam regulations of the Norwegian University of Science and Technology (NTNU).

Kristoffer Moen (Sign.)  
Trondheim June 9, 2014

---





# Contents

Abstract . . . . .	i
Preface . . . . .	v
<b>1 Introduction</b>	<b>1</b>
1.1 Process . . . . .	2
1.2 Objective . . . . .	3
1.3 Literature Review . . . . .	3
1.4 Thesis Structure . . . . .	4
<b>2 Process Description</b>	<b>5</b>
2.1 Preheating and Sulfur Removal . . . . .	5
2.2 Pre-reformer . . . . .	5
2.3 Synthesis gas production . . . . .	7
2.3.1 Steam Methane Reforming . . . . .	7
2.3.2 Autothermal Reforming . . . . .	8
2.3.3 Ceramic Membrane Reforming . . . . .	9
2.3.4 Synthesis Gas Applications . . . . .	9
2.4 Fischer Tropsch . . . . .	10
2.4.1 Product Selectivity . . . . .	11
2.4.2 Gas Loop Design . . . . .	12
2.5 Product Upgrading . . . . .	12
2.6 Hydrogen Plant . . . . .	13
2.7 Heat Integration . . . . .	14
<b>3 Kinetic Model</b>	<b>17</b>
3.1 Model Implementation . . . . .	20
3.2 Model Limitations . . . . .	23
<b>4 Simulation Model</b>	<b>25</b>
4.1 Base Case Configuration . . . . .	25

4.2	Configuration 1 . . . . .	27
4.3	Configuration 2 . . . . .	29
4.4	Heat Integration . . . . .	29
<b>5</b>	<b>Results and Discussion</b>	<b>33</b>
5.1	Base Case Configuration . . . . .	33
5.2	Main Analysis . . . . .	38
5.3	Heat Integration . . . . .	45
5.3.1	Base Case Configuration . . . . .	45
5.3.2	Configuration 2 . . . . .	49
5.3.3	Configuration Comparison . . . . .	52
5.4	Future work . . . . .	52
<b>6</b>	<b>Conclusion</b>	<b>55</b>
	<b>Bibliography</b>	<b>56</b>
<b>A</b>	<b>MATLAB Kinetic Script</b>	<b>59</b>
<b>B</b>	<b>DLL Extension code for pentene</b>	<b>63</b>
<b>C</b>	<b>MATLAB to HYSYS Implementation Data</b>	<b>71</b>
<b>D</b>	<b>Pinch analysis: Base Case Configurartion</b>	<b>73</b>
<b>E</b>	<b>Pinch analysis: Configurartion 2</b>	<b>77</b>

# List of Figures

1.1	Block diagram of a GTL-plant where the main processes are included.	2
2.1	Main flowsheet for a conventional GTL plant	6
2.2	Closed gas loop design: external and internal recycle of tail gas, adapted from [3].	13
2.3	Flowsheet of a modern Hydrogen Plant, adapted from [4]	14
2.4	A simplified block diagram describing the different heat inputs and outputs of a process.	15
3.1	An illustration of the CO-insertion mechanism that forms the chain starter (CH <sub>3</sub> -S).	18
3.2	Chain growth probability ( $\alpha_n$ ) plotted against increasing carbon number. Calculated from the MATLAB script presented in Appendix A.	21
3.3	Calculated production rates for alkanes and alkenes at $T=200$ [°C], $P=1.5$ [MPa], $H_2/CO = 2.1$ using the MATLAB script presented in Appendix A.	21
3.4	An illustration on how the extension code is sent to the Aspen-Tech HYSYS V8.0 software. The EDF file is the link between the extension code and the software.	23
4.1	The first of two new GTL-configurations that will be simulated: Configuration 1. A CO <sub>2</sub> rich tail gas from the hydrogen plant will be utilized for synthesis gas production. It will also be distributed along the PFR reactor to adjust the H <sub>2</sub> /CO ratio to a desired value.	28
4.2	The second new GTL-configuration where one large reactor have been divided into three smaller ones: Configuration 2. Both water and products are separated between each of the reactors to improve the overall efficiency.	31

5.1	The resulting temperature profile along the 12 meter long PFR reactor in the Base Case Configuration. . . . .	35
5.2	A plot displaying the main component mol fractions changes along the 12 meter long PFR reactor. The result is collected from the Base Case Configuration. . . . .	36
5.3	A plot displaying the weight fraction changes through the 12 meter long PFR reactor. All the data is gathered from the Base Case Configuration. . . . .	36
5.4	The resulting temperature profile along the 12 meter long PFR reactor, Configuration 1. It is also included how the H <sub>2</sub> /CO ratio was adjusted with pure hydrogen to a level of 1.6 along the reactor length. . . . .	40
5.5	The initial heat and cooling demand for the Base Case Configuration.	46
5.6	The proposed heat-exchanger network for Base Case Configuration. The grid was design below a pinch temperature of 1000°C. . . . .	47
5.7	The proposed heat-exchanger network for Configuration 2. The grid was designed below a pinch temperature of 1000°C. . . . .	50

# List of Tables

2.1	The different synthesis gas-to-syncrude processes with their desired $H_2/CO$ ratio. . . . .	9
2.2	Most commonly used catalyst in the Fischer Tropsch synthesis with it's corresponding $\alpha$ values and main products.[5] . . . . .	11
3.1	The elementary steps that was included in deriving the kinetic model by Todic et al.[2]. . . . .	18
3.2	All kinetic parameters that was used to calculate the given reaction rates and equilibrium constants for the Todic et al.[2] kinetic model	22
3.3	Reaction rate comparison test for MATLAB and HYSYS at six different process conditions. . . . .	23
4.1	The feedstock for the different simulations: Natural gas with its related mol fractions. . . . .	26
4.2	The main specifications of the Fischer-Tropsch reactor regarding overall design, cooling and choice of catalyst size. . . . .	26
5.1	$H_2/CO$ ratio and temperature response out of the ATR when increasing each of the inlet streams individually. . . . .	34
5.2	Final amount and process conditions for the three inlet flows in the Base Case Configuration: Natural gas, Oxygen and Steam. . .	34
5.3	The final production amounts in the Base Case Configuration. This included both alkanes and alkenes, $C_1$ to $C_{15}$ . . . . .	37
5.4	The kinetic responce for the Fischer-Tropsch synthesis when increasing the $H_2/CO$ ratio in the synthesis inlet, pressure and total tube reactor volume individually. . . . .	37
5.5	The final pressure swing absorber (PSA) tail gas composition. . . .	38
5.6	Main results comparison for the different configurations: Base Case, Configuration 1 and 2 . . . . .	39

5.7	The product distribution for each of the configurations: Base Case, Configuration 1 and 2. This included the mol flows for alkanes, alkenes and the total amount. . . . .	41
5.8	Flow distributions for the different process configurations: Base Case, Configuration 1 and 2. . . . .	44
5.9	Heat integration results for the Base Case Configuration. . . . .	48
5.10	Heat integration results: Base Case Configuration and Configuration 2. . . . .	52
C.1	Alkanes reaction rates comparison between MATLAB and HYSYS	71
C.2	Alkenes reaction rates comparison between MATLAB and HYSYS	72
D.1	Average heat-capacity flow rate values : Base Case Configuration.	73
D.2	Ranked order of the different temperature intervals for the Base Case Configuration. The energy balances for each of the intervals are also included. . . . .	74
D.3	Main pinch analysis table for the Base Case Configuration. . . . .	74
E.1	Average heat-capacity flow rate values: Configuration 2. . . . .	77
E.2	Ranked order of the different temperature intervals for Configuration 2. The energy balances for each of the intervals are also included. . . . .	78
E.3	Main pinch analysis table for Configuration 2. . . . .	78

# Nomenclature

$A$	Preexponential factor for rate constant for elementary step $i$ [MPa <sup>-1</sup> ]
$c$	Constant determining chain length dependence
$C_p$	Average specific heat capacity [kJ kg <sup>-1</sup> °C <sup>-1</sup> ]
$CP$	Average heat capacity flow [kW °C <sup>-1</sup> ]
$E_i$	Activation energy for elementary step $i$ [kJ mol <sup>-1</sup> ]
$F_0$	Total amount of natural gas entering the system which can be processed to final products (C <sub>5+</sub> )
$H$	Enthalpy [kJ mol <sup>-1</sup> ]
$k_i$	Reaction rate constant for elementary step $i$
$K_i$	Equilibrium constant for elementary step $i$
$m$	Mass flow rate [kg s <sup>-1</sup> ]
$P$	Pressure [MPa]
$P_i$	Partial pressure of species $i$ [MPa]
$Q$	External energy input [kW]
$R$	Universal gas constant [kJ kmol <sup>-1</sup> K <sup>-1</sup> ]
$R_i$	Reaction rate of species $i$ [mol g <sub>cat</sub> <sup>-1</sup> h <sup>-1</sup> ]
$S$	Vacant active site on catalyst
$T$	Temperature [°C]
$T_{\text{int}}$	Temperature interval
$\#$	Numbers of

## *Greek Symbols*

$\Delta T_{\text{min}}$	Minimum temperature difference between cold and hot stream
$\Delta H$	Enthalpy difference in elementary step $i$ [kJ mol <sup>-1</sup> ]
$\alpha_n$	Chain growth probability for carbon number $n$
$\chi$	Composition molar fraction
$\omega$	Composition weight fraction

*Acronyms*

ASF	Anderson, Schultz and Flory
ASU	Air Separation Unit
ATR	Auto Thermal Reformer
C	Cooler
CMR	Ceramic Membrane Reforming
DLL	Dynamic link library
EDF	Extension definition file
F-T	Fischer-Tropsch
FTR	Fisher Tropsch Reactor
FTS	Fischer Tropsch Synthesis
GTL	Gas-to-liquid
H	Heater
HDS	Desulfurization
HTSC	High Temperature Shift Converter
HTER	Haldor Topsøe Exchange Reformer
HTFT	High Temperature Fischer Tropsch
LTFT	Low Temperature Fischer Tropsch
RDS	Rate determining step
SMR	Steam methane reformer
WBH	Waste Heat Boiler

*Subscripts*

cal	Calculated
exp	Experimental value
$n$	number of carbon atoms



# Chapter 1

## Introduction

Today most engine fuels are being processed from petroleum oil, although the availability of this feedstock is considerably less than both coal and methane.[6] This is where the gas-to-liquid (GTL) plant is introduced. A gas-to-liquid plant consists of converting gaseous carbon based feedstock into more valuable products like engine fuels and chemicals. One of the main technologies on this subject is the Fischer-Tropsch synthesis (FTS). There are also other technologies available to convert synthesis gas to synthetic crude oil (syncrude) but FTS is the most commonly used method.[3]

This process was developed by the German scientists Franz Fischer and Hans Tropsch during World War II. Their intention was to fulfil the required demand for transportation fuel. A production of 600 000 ton/year was achieved with the use of coal gasification.[5]

There have been made recent improvements to the Fischer-Tropsch (F-T) technology which have increased the interest for this production method. The opportunity to utilize remote gas resources to produce more valuable products are highly desirable.[1] The process favors the production of linear alkanes instead of aromatic compounds which are highly desirable for diesel production due to the high cetane numbers.[3]

The main challenge with this production method is the high capital cost for producing synthesis gas. The synthesis gas production constitutes 40 % of the total investment cost for a complete GTL-plant. It is therefore necessary to do more research in order to find a more efficient and optimal process configuration of synthesis production. These contributions could reduce the overall cost to a

lower level.[7]

There are a lot of interesting research being done regarding GTL-relevant subjects such as the synthesis gas production configuration[1] and Fischer-Tropsch catalysts[8]. The main focus of this project however will concern the overall process design of a GTL-plant. There are little available research being reported regarding this subject, which makes the results from this project highly interesting.

## 1.1 Process

A GTL-plant consist of three main sections: synthesis gas (syngas) production, Fischer-Tropsch synthesis and upgrading of products. A block diagram of this process is presented in Figure 1.1.

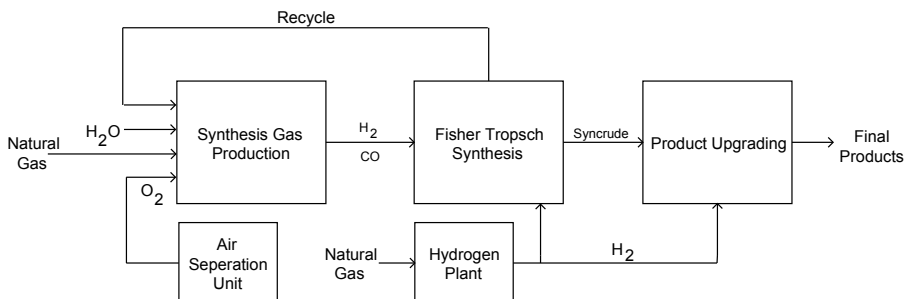


Figure 1.1: Block diagram of a GTL-plant where the main processes are included.

In the synthesis gas production, natural gas is converted to a mixture of carbon monoxide and hydrogen in various ratios. This gas is then introduced to a Fischer-Tropsch (F-T) reactor where a wide range of hydrocarbons are produced, called syncrude. There is often introduced a recycle stream in this step to enhance the overall conversion of feedstock. The last step in a GTL-plant is the product upgrading process which fulfils the desired specification for a given product.[1][3]

All of these process stages are explained in greater detail in Chapter 2.

## 1.2 Objective

The main objective of this project is to find an optimal gas-to-liquid process configuration that favors the production of longer hydrocarbons chains ( $C_{5+}$ ). The carbon and heat efficiency are the main parameters that are desirable to maximize. These are defined by:

- Carbon Efficiency: Number of carbons in product divided by number of carbons entering the system ( $C_{\text{Prod}} / (C_{\text{Feed}} + C_{\text{Fuel}})$ ).
- Energy Efficiency: Amount of energy present in the product stream divided by total energy input into the system. ( $E_{\text{Prod}} / (E_{\text{Feed}} + Q)$ )

The first task involves implementing an accurate model to describe the F-T product distribution in the AspenTech process simulation software 'HYSYS V8.0'. A new kinetic model published by Todić et al. [2] was chosen for this description because the model proved consistent with reported measurements. The model includes production of both alkanes and alkenes and has a product selectivity that depends on both composition, temperature and pressure. When this model is successfully implemented the different simulations can begin.

There are in total three different cases that will be simulated and compared with each other. The initial configuration will be a conventional gas-to-liquid plant which is referred to as the Base Case Configuration. The two other Configurations are called respectively Configuration 1 and 2. Lower  $H_2/CO$  ratio, hydrogen distribution and multiplereactors in series are some of the changes made in these two configurations. All details regarding these configurations and process conditions are presented in Chapter 4. The results from these two will be compared with the Base Base Configuration in order to find which of the designs favors the production of longer hydrocarbon chains. One of the proposals in this project is to utilize tail gas stream from the hydrogen plant in the synthesis gas production. This stream consists of large amount of  $CO_2$  which would be desired to convert to final products, which would also reduce emissions.

## 1.3 Literature Review

The main database for literature collection in this project have been Scopus, by Elsevier. This was used due to the large availability of relevant articles for this project. The main keyword for the literature search was: *Gas-to-liquid plant, Fischer-Tropsch, Synthesis gas production and cobalt*.

The article "CO-insertion mechanism based kinetic model of the Fischer-Tropsch synthesis reaction over Re-promoted CO catalyst" by Todić et al.[2] was used to describe the overall kinetic model for the Fischer-Tropsch Synthesis.

There have also been used two books to describe the overall process description. The book "Chemical Process Technology" by Moulijn et al.[9] was used to specify proper process conditions for hydrogen and synthesis gas production. For the Fischer-Tropsch synthesis "Fischer-Tropsch Refining" by de Klerk et al.[3] was used to simulate accurate process design and conditions.

## 1.4 Thesis Structure

Chapter 2 presents the process description of a gas-to-liquid plant. This includes the production of synthesis gas, the Fischer-Tropsch synthesis, and other relevant topics for a GTL plant. In Chapter 3, the selected Fischer-Tropsch synthesis kinetic model description is included. This includes the derivation of the kinetic model together with how the model was implemented into the AspenTech HYSYS process simulation software. Details of different process configurations are then included in Chapter 4, called Simulation Procedure. The final evaluation of results are included in Chapter 5. Recommendations regarding future work are also included in this chapter. Chapter 6 contains the final conclusion of this report.

One of the main challenges with this project is the many degrees of freedom in the process. *Reactor size, stream amounts, temperature and pressure* are just some of the variables that could be altered in each of the simulations. Therefore, every effort has been made to ensure that the report is as structural and clear as possible.

## Chapter 2

# Process Description

Longer hydrocarbon chains ( $C_{5+}$ ) are being produced from natural gas. A general flowsheet of this process is presented in Figure 2.1. The different steps in this conventional GTL-plant will be explained in more detail in the proceeding sections.

### 2.1 Preheating and Sulfur Removal

There is a need to remove sulfur and other hetero-compounds (N,O,etc.) from a given feedstock. These compounds acts like poison that would deactivate the catalyst rapidly. The process is called hydrodesulfurization (HDS) where added hydrogen breaks the C-S bond and sulfur is separated out as  $H_2S$ . The sulfur content after this step should not exceed 1 ppm. For this process to occur the process temperature should be around  $400^{\circ}C$ . Preheating of the inlet feeds is achieved with the of a fired heater that uses natural gas as an energy source to fulfil the needed energy increase in the feed. After these steps, natural gas is mixed with steam or  $CO_2$  before entering the pre-reformer.[9]

### 2.2 Pre-reformer

Natural gas mainly consists of methane, but also small amounts of higher hydrocarbons like ethane and propane. Because of this it is desirable to install a pre-reformer before the main reforming unit. A pre-reformer is a catalytic fixed

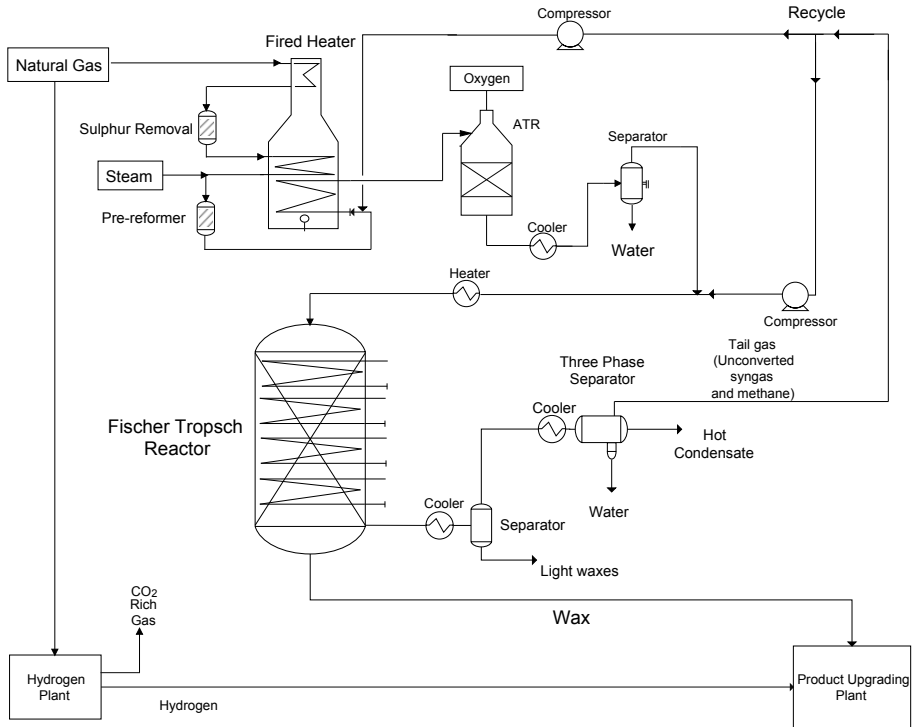
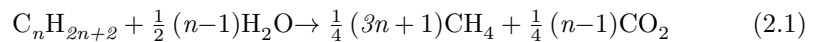


Figure 2.1: Main flowsheet for a conventional GTL plant

bed reactor operating adiabatically at about  $500^{\circ}\text{C}$ . In this temperature range higher hydrocarbons are converted to methane and carbon dioxide according to reaction 2.1.

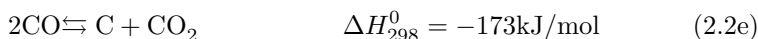
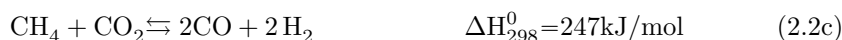


The most important advantage of including a pre-reformer is that it reduces the chance of carbon deposition later in the process. With higher temperature levels the probability for carbon formation also increases.[9]

## 2.3 Synthesis gas production

The synthesis gas production unit converts a carbon feedstock into a mixture of hydrogen and carbon monoxide in various ratios. The choice of raw materials is determined by cost and availability, but most importantly by what the synthesis gas will be used for. Natural gas is the main feedstock of choice for a GTL-plant.[9]

Main reactions for synthesis gas production are presented in Equations (2.2a-i). For reforming methane with the use of steam the main reactions are the steam reforming reaction (2.2a) and the water-gas shift reaction (2.2b). When methane reacts with CO<sub>2</sub> reaction 2.2c it is referred to as "dry reforming" since no steam is present. Methane can also undergo degradation which results in coke, reaction (2.2d) and (2.2e). These reactions are highly undesirable due to rapid deactivation of the catalyst activity. Other reactions (2.2f)-(2.2i) describe both partial and complete oxidation of methane when oxygen is present in the reforming vessel.[9]



Synthesis gas production methods that are used in GTL-plants will now be explained in detail.

### 2.3.1 Steam Methane Reforming

This production method uses steam to convert natural gas to synthesis gas. Due to the high stability of methane, both high temperatures ( $> 750^\circ\text{C}$ ) and nickel supported catalysts are required for the reaction to take place. The main reactions that occur in this section are steam methane reforming and water gas shift

reaction, see reactions (2.2a) and (2.2b). Reforming reactions are endothermic, meaning that energy have to be introduced into the system. This energy demand is supplied by combustion of fuel outside reformer tubes. Typically this fuel would be some kind of natural gas. Heat present in the tail gas from this combustion is used to preheat inlet streams and make superheated steam. There is also a possibility to replace some of the entering steam with  $\text{CO}_2$ . This replacement depends on the desired  $\text{H}_2/\text{CO}$  ratio for for the downstream processes. A typical industrial steam reforming unit could consist of 500-600 tubes with a length up to 12 meters.[9]

### 2.3.2 Autothermal Reforming

The most promising technology related to efficiency and economy is Autothermal Reforming (ATR). An ATR consists of a burner, a combustion chamber and a catalyst bed located inside a refractory-line steel vessel.[7] Natural gas, steam and oxygen are injected into the combustion zone where partial and complete oxidation of methane occur at about 1900 °C, reaction (2.2f) and (2.2g). Unconverted methane continues through the reactor and enters the reforming zone where catalytic reforming takes place, reactions (2.2a) and (2.2c). Energy needed in the reforming reactions are supplied by the exothermic oxidation reactions.[9]

All large-scale industrial processes of Fisher-Tropsch technologies uses pure oxygen for producing synthesis gas. This requires that an air separation unit (ASU) is included in the process. The overall efficiency would decrease rapidly if air was used due to the high content of  $\text{N}_2$ , 78%. The required reforming volume would also increase enormously due to this effect. The cost of investing and operating an ASU is one of the biggest weaknesses of  $\text{O}_2$  blown ATRs.[3] These units are also large in size and have a high capital cost which could limit the capacity of the overall plant. Finding a configuration that gives a reduction in oxygen consumption is therefore highly desirable. A higher inlet temperature and lower outlet temperature would reduce the oxygen demand. Low outlet temperature will produce a synthesis gas with higher  $\text{H}_2/\text{CO}$  ratio. The desired ratio for Fischer-Tropsch synthesis is roughly 2, and by replacing steam with  $\text{CO}_2$  in the ATR this ratio could be reached.[7]

The manufacturer Topsøe has designed an exchange reformer (HTER) that is coupled together with an ATR. Energy that is produced from the ATR is used for steam reforming and to pre-heating the feed in the HTER, a combination thats results in an overall decrease of oxygen consumption. These configurations are operating at Sasols's facilities in South Africa with excellent operating records and that show lower  $\text{O}_2$  consumption than single ATR configurations. Another



method for reducing the oxygen demand are to include a steam reformer before the ATR reformer. This configuration reduces the operating cost while still producing the desired  $H_2/CO$  ratio.[7][9]

### 2.3.3 Ceramic Membrane Reforming

New technologies are also being evaluated to produce synthesis gas in a more effective manner. The most promising technology today is ceramic membrane reforming (CMR). In this process, air is injected at one side of the membrane where only 100 % oxygen passes through. This stream can further react with the hydrocarbons to produce synthesis gas. With this configuration, the need for pure oxygen is avoided and no air separation unit has to be included. There are still major challenges regarding the stability of the membrane during operation which have to be resolved for this technology to be reliable and functional.[7]

### 2.3.4 Synthesis Gas Applications

There are various processes that use synthesis gas as their main feedstock. The main parameter in the synthesis gas is the  $H_2/CO$  ratio, and the stoichiometric reaction in the specific process decides what the ratio should be. Some of these processes with their synthesis gas mixture requirements are presented in Table 2.1.

Table 2.1: The different synthesis gas-to-syncrude processes with their desired  $H_2/CO$  ratio.

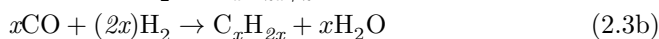
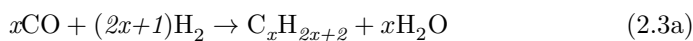
<b>Application</b>	<b>Desired <math>H_2/CO</math> Ratio</b>
Aldehydes	1 : 1
Fisher Tropsch	2 : 1
Methanol/Higher alcohols	2 : 1
Ammonia	3 : 1

Most synthesis applications require a high pressure. Methanol for example is produced at 50-100 bar. Due to this effect most steam reformers operate at high pressure. The advantages are lower synthesis gas compression cost later in the process together with a smaller reformer size. A major setback is increasing methane slip with increasing pressure (less methane get converted). It is economically beneficial to operate at the highest possible pressure since the cost of excess compression work significantly outbalances the cost of less converted

methane. The effect of less converted methane is counteracted by increasing the reaction temperature and by adding excess steam in the reformer. This shifts the equilibrium so that more product is produced and methane slip is reduced significantly.[9]

## 2.4 Fischer Tropsch

The Fischer Tropsch (F-T) process converts synthesis gas ( $\text{CO}+\text{H}_2$ ) to hydrocarbons. F-T synthesis involves a large number of products and intermediates but alkanes and alkenes are the main products, see reaction (2.3a) and (2.3b):[5]



These reactions are highly exothermic, hence heat removal is a crucial design parameter for the specific reactor type. The temperature level determines which reactor is most beneficial for producing a specific product. When desired products are gasoline and chemicals, the most used reactor type is the gas-fluidized bed reactor, operating at a temperature of  $350^\circ\text{C}$  or above. This process is referred to as high-temperature F-T synthesis (HTFT). However, if wax is the desired product, multitubular fixed bed reactor (PFR) or slurry bubble column reactor types are preferable. These reactors operate in temperature ranges of  $220^\circ\text{C}$ , referenced as low temperature F-T (LTFT).[5]

Products leave the PFR reactor in two different streams. One of the streams is in the liquid phase consisting of wax while the other is in the vapour phase consisting of unconverted synthesis gas and lighter syncrude components. The vapour phase is cooled down to roughly  $100^\circ\text{C}$  where hot condensate is removed. This condensate consist of lighter wax components and should therefore not be cooled lower than its congealing point. To recover the unconverted synthesis gas present in the vapour phase is stepwise cooling introduced. The remaining components are then processed in a three phase separator where water, cold condensate (light oils) and tail gas are separated from each other. This syncrude recovery section is shown in Figure 2.1.[3]

Iron and cobalt are the most commercially used catalysts in the F-T process. The product selectivity and choice of catalyst will be outlined in the following section.[5]

### 2.4.1 Product Selectivity

Carbon distribution in the Fischer-Tropsch synthesis is determined by the probability of chain growth on the catalyst, also called the  $\alpha$ -value. The product distribution is often explained by a statistical distribution called Anderson, Schultz, and Flory (ASF), given by:

$$\omega_i = i(1 - \alpha)^2 \alpha^{i-1} \quad (2.4)$$

where  $i$  is the number of carbon atoms, and  $\omega_i$  is the weight fraction of a component with length  $i$ . Probability for the chain to terminate is explained by  $1-\alpha$ . Chain length of hydrocarbons depend on the nature of the catalyst and the chosen process conditions. If longer chains are desired, it is beneficial to decrease the  $H_2/CO$  ratio and the temperature while increasing the pressure level. The main catalysts that can be used in the Fischer Tropsch process are presented In Table 2.2 with their corresponding  $\alpha$  value and main product.[5]

Table 2.2: Most commonly used catalyst in the Fischer Tropsch synthesis with it's corresponding  $\alpha$  values and main products.[5]

Catalyst	$\alpha$	Main product
Nickel	Low	Methane
Iron	0.65-0.70	Gasoline
Cobalt	0.75-0.85	Waxes

It has been difficult to find an exact FTS mechanism for explaining the complex kinetic that occur. This is mainly due to the many products and surface intermediates.[2] This explains why in practice there are some deviations from the ASF distribution. The major distribution deviation is related to the production rates of methane and  $C_2$ . The actual production of methane is usually higher than the predicted value given by the ASF distribution, while the  $C_2$  production rates are considerably lower. One way of improving the distribution in LTFT synthesis is by the use of two  $\alpha$ -values. In this case the first  $\alpha$ -value ( $\alpha_1$ ) describes the distribution for  $C_8$  and lower while  $\alpha_2$  describes the distribution of  $C_{12}$  and higher. The distribution for  $C_9-C_{11}$  are explained by different contributions.[3]

Various mechanisms have been suggested to explain the F-T synthesis reactions. New research investigation have identified two main mechanism as the the most probable, called carbide and CO-insertion. The main difference between these two is in which sequence the chain starter ( $CH_3-S$ ) is formed. In the carbide

mechanism, C-O bond is severed before C is hydrogenated, while the CO mechanism is based on C-O breakage after hydrogenation steps.[2]

Storsæter et. al [10] has compared these two mechanisms and concluded that the C-O mechanism is likely the main mechanism for the Fisher Tropsch synthesis. This conclusion was based on several tests showing that the CO-insertion mechanism had a lower energy barrier than the carbide mechanism. In Chapter 3 will the CO-insertion mechanism be explained in more detail. Regardless of which mechanism is used, the growth of hydrocarbon chains occur by stepwise addition of single carbon molecule derived from CO in the present synthesis gas.

### 2.4.2 Gas Loop Design

There are numerous ways to distribute the unconverted synthesis gas flow around the Fischer-Tropsch synthesis. The choice of a gas loop design has a large influence on the system. It determines the flow and distribution of the unconverted synthesis gas and has a large impact on the overall carbon efficiency. The carbon efficiency is desirably as high as possible, indicating that the gas loop design is actually an optimization problem. There are two main designs for these kind of loops: open and closed. The difference is related to whether the tail gas from the product recovery section undergoes further processing or not. In a pure open loop gas design, no tail gas is being recycled meaning that all the unconverted synthesis gas is lost. When the tail gas is recycled back to the F-T synthesis the process is refereed to as closed. This design is more desirable since this enhances the overall efficiency significantly.[3]

There are two different variates for the closed design: internal and external recycle. A representation of these designs are included in Figure 2.2. When the the tail gas is sent directly to the Fischer-Tropsch synthesis without any separation it is termed an internal recycle. However, it is an external recycle if the tail gas undergoes any form of separation step and/or conversion unit before being recycled. The complexity of including an internal recycle is significantly lower than for an external recycle. An external recycle design could require new utilities to be included for processing of the tail gas amount.[3]

## 2.5 Product Upgrading

Products from the low temperature Fischer-Tropsch synthesis ( $C_{5+}$ ) need further processing before they can be used as products, for example high quality

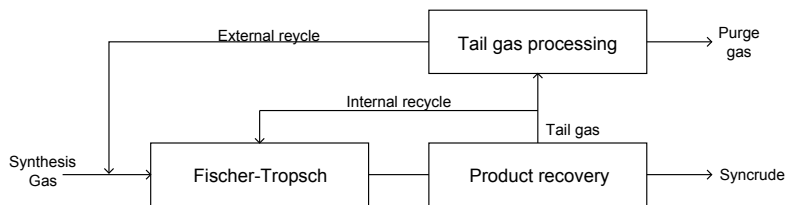


Figure 2.2: Closed gas loop design: external and internal recycle of tail gas, adapted from [3].

diesel. This process is referred to as isomerization. During this process the overall structure of a molecule is changed without changing the molecular weight. The objective is to adjust the quality of the products to their desirable properties.[3][9]

## 2.6 Hydrogen Plant

A hydrogen plant is necessary for a refining plant to function. This hydrogen amount will be used for both sulfur removal and upgrading of the hydrocarbon products.[4] Older hydrogen plants consists of a steam methane reformer (SMR) that converts the hydrocarbon feed to a syngas mixture. The relevant description of this production method is included in subsection 2.3.1. The combination of a high temperature converter (HTSC) and low temperature shift converter (LTSC) shifts the CO to hydrogen, see equation 2.2b. The produced amount is subsequently sent to a CO<sub>2</sub> removal unit followed by a methanation step which converts the remaining CO and CO<sub>2</sub> to methane and water. With this configuration a product gas contains normally 95 – 97% hydrogen.[4]

In recent years large technology enhancements have been made in the field of hydrogen purification. The CO<sub>2</sub> removal unit and methanation step are now replaced by a pressure swing adsorption unit. This change together with other design and technology improvements have resulted in a product stream with purity of typically 99.99 %, of hydrogen.[4] The absorption unit operates with rapid cycles due to isothermal operation, reducing vessel size and lowering capital cost for the unit. The absorbent is regenerated by reducing pressure inside the vessel as indicated by the name of the unit. An industrial size PSA normally requires 4 to 12 absorbent vessels in combination to process the required amount.[11]

A general flowsheet of a modern hydrogen plant is presented in Figure 2.3.

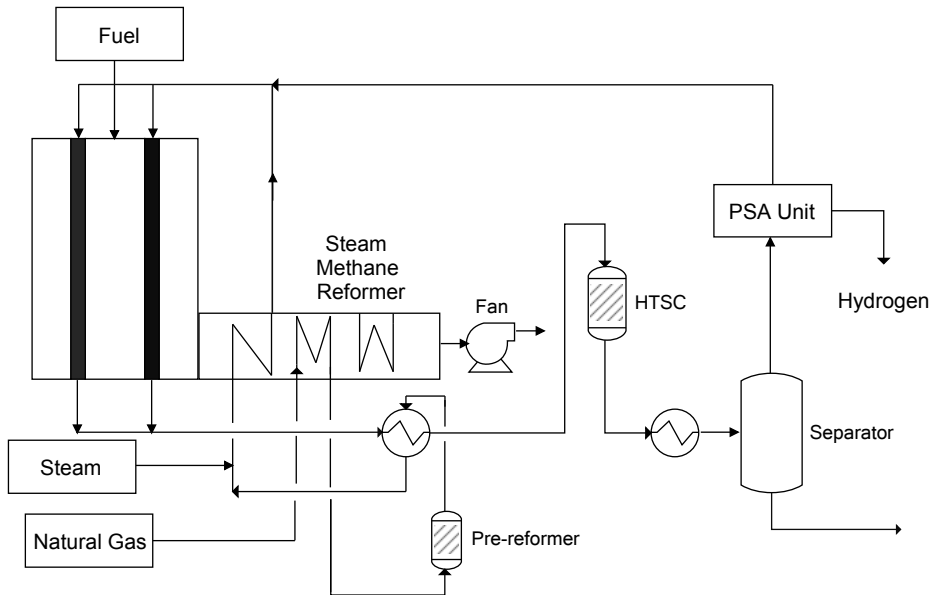


Figure 2.3: Flowsheet of a modern Hydrogen Plant, adapted from [4]

## 2.7 Heat Integration

The energy output of a system is in this thesis referring to the energy present in the product together with any electrical power production in the process. The energy input is determined by energy in feedstock together with the added energy,  $Q$ . Overall block diagram of this is presented in Figure 2.4.

The energy efficiency of a given system is defined as the energy output divided by the energy input, and it is desirable to maximize this value for the process to be economical. This energy improvement can be achieved by enhancing the feedstock conversion or electrical power generation, or by reducing the external energy input ( $Q$ ). Improvement of the energy efficiency is fulfilled by evaluating the possibly to utilize available energy in the process. A process have often multiple hot and cold streams which need cooling or heating. This is where the

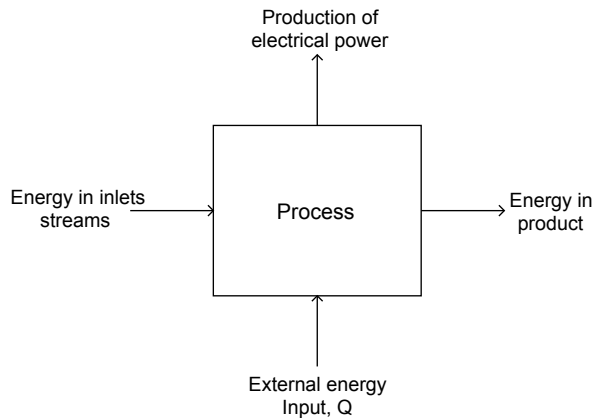


Figure 2.4: A simplified block diagram describing the different heat inputs and outputs of a process.

heat integration comes into play. By finding an optimal heat exchanger network design, the external energy input could be reduced. It is necessary to include a minimum temperature difference between hot and cold streams,  $\Delta T_{\min}$ .  $10^{\circ}\text{C}$  or higher is required for the design to be functional.[11]

For multiple streams this design would be rather complex where different designs would be considered feasible. The most commonly used method for this energy minimizing analysis is called "pinch-analysis". There is a pinch between hot and a cold stream when temperature versus heat is plotted. This specific temperature separates the system into two different thermodynamic regions and is where the thermodynamic constrains for the system occurs. Heat should never be transferred across this point. One method for finding pinch temperature is called the "Problem Table Method".[11] This is a numerical method with the following procedure:

1. Convert the actual stream temperature ( $T_{\text{act}}$ ) into temperature interval by these to expressions:

$$\text{hot streams } T_{\text{int}} = T_{\text{act}} - \frac{\Delta T_{\min}}{2}$$

$$\text{cold streams } T_{\text{int}} = T_{\text{act}} + \frac{\Delta T_{\min}}{2}$$

2. Sort the different temperature intervals

3. Calculate a heat balance for included process streams in each of the temperature intervals:

$$\Delta H_n = (\sum CP_c - \sum CP_h)(\Delta T_n)$$

where

$\Delta H_n$  = net heat required in  $n^{th}$  interval [kW]

$CP$  = Heat-capacity flow rate =  $m \times C_p$  [kW °C<sup>-1</sup>]

$m$  = mass flow rate [kg/s]

$C_p$  = average specific heat capacity from the source temperature ( $T_s$ ) to target temperature ( $T_t$ ) [kJ kg<sup>-1</sup>°C<sup>-1</sup>]

$\sum CP_c$  = Sum of the heat capacities of all the cold streams in the temperature interval [kW °C<sup>-1</sup>]

$\sum CP_h$  = Sum of the heat capacities of all the hot streams in the temperature interval [kW °C<sup>-1</sup>]

$\Delta T_n$  = interval temperature difference = ( $T_{n-1} - T_n$ ) [°C]

4. Cascade the heat surplus from one interval to the next down the column of interval temperatures.
5. Introduce just enough heat on the top of the cascade to eliminate all negative values.

The pinch temperature occurs where the heat flow in the cascade is zero and the heat exchanger configuration should be designed around this single parameter. If the heat exchange occurs below the pinch,  $CP_h \geq CP_c$  needs to be fulfilled. Above pinch  $CP_h \leq CP_c$  is the requirement. If a specific stream has not reached the desired temperature an external heater should be included above the pinch. External cooling is needed below the pinch.[11]



# Chapter 3

## Kinetic Model

Fischer Tropsch synthesis consist of complex reactions which results in a large range of products like alkanes, alkenes and oxygenates as described in section 2.4. Todic et al. [2] have proposed a kinetic model which is explained by the CO-insertion mechanism. Their kinetic analyses focused on hydrocarbon production of C<sub>1</sub>-C<sub>15</sub> alkanes and C<sub>2</sub>-C<sub>15</sub> alkenes. This section presents the model-derivation, assumptions and production rates from their article. The implementation steps of the model are also included.

### Model Derivation

The model is based on rhenium promoted cobalt as catalyst due to its high activity and selectivity to produce higher hydrocarbons (wax). Production of other side products like oxygenates were neglected due to their lower production rates. The kinetic model has a probability value ( $\alpha_i$ ) that depends on temperature, pressure and composition of the feed. This implementation shows promising results when comparing it with actual process data. The CO-insertion mechanism can be divided into several steps. CO and H<sub>2</sub> will first be adsorbed on the catalyst surface. Then the adsorbed CO undergoes stepwise hydrogenation to form the chain starter (CH<sub>3</sub>-S). This is presented in Figure 3.1.

The chain starter will then undergo propagation before leaving the catalyst as products (termination). A detailed description of all of the elementary steps that constitute the overall CO-insertion mechanism are presented in Table 3.1. Parameter S expresses the fraction of free active sites on the catalyst.

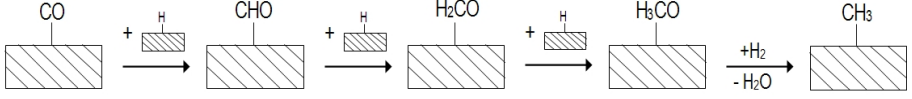


Figure 3.1: An illustration of the CO-insertion mechanism that forms the chain starter ( $\text{CH}_3\text{-S}$ ).

Table 3.1: The elementary steps that was included in deriving the kinetic model by Todic et al.[2].

No.	Elementary Step	Rate and equilibrium constants
(1)	$\text{CO} + \text{S} \leftrightarrow \text{CO-S}$	$K_1$
(2)	$\text{H}_2 + 2 \text{S} \leftrightarrow 2\text{H-S}$	$K_2$
(3 <sup>RDS</sup> )	$\text{CO-S} + \text{H-S} \rightarrow \text{CHO-S} + \text{S}$ $\text{CO-S} + \text{CH}_3\text{-S} \rightarrow \text{CH}_3\text{CO-S} + \text{S}$ $\text{CO-S} + \text{C}_n\text{H}_{2n+1}\text{-S} \rightarrow \text{C}_n\text{H}_{2n+1}\text{CO-S} + \text{S} \quad n=2,3,\dots$	$k_3$
(4)	$\text{CHO-S} + \text{H-S} \leftrightarrow \text{CH}_2\text{-S} + \text{S}$ $\text{CH}_3\text{COO-S} + \text{H-S} \leftrightarrow \text{CH}_3\text{CHO-S} + \text{S}$ $\text{C}_n\text{H}_{2n+1}\text{CO-S} + \text{H-S} \leftrightarrow \text{C}_n\text{H}_{2n+1}\text{CHO-S} + \text{S} \quad n=2,3,\dots$	$K_4$
(5)	$\text{CH}_2\text{O-S} + 2\text{H-S} \leftrightarrow \text{CH}_3\text{-S} + \text{OH-S} + \text{S}$ $\text{CH}_3\text{CHO-S} + 2\text{H-S} \leftrightarrow \text{CH}_3\text{CH}_2\text{-S} + \text{OH-S} + \text{S}$ $\text{C}_n\text{H}_{2n+1}\text{CHO-S} + 2\text{H-S} \leftrightarrow \text{C}_n\text{H}_{2n+1}\text{CH}_2\text{-S} + \text{OH-S} + \text{S} \quad n=2,3,\dots$	$K_5$
(6)	$\text{OH-S} + \text{H-S} \leftrightarrow \text{H}_2\text{O} + 2\text{S}$	$K_6$
(7 <sup>RDS</sup> )	$\text{CH}_3\text{-S} + \text{H-S} \rightarrow \text{CH}_4 + 2\text{S}$ $\text{C}_n\text{H}_{2n+1}\text{-S} + \text{H-S} \rightarrow \text{C}_n\text{H}_{2n+2} + 2\text{S}$	$k_7$
(8 <sup>RDS</sup> )	$\text{C}_2\text{H}_5\text{-S} \rightarrow \text{C}_2\text{H}_4 + \text{H-S}$ $\text{C}_2\text{H}_{2n+1}\text{-S} \rightarrow \text{C}_n\text{H}_{2n} + \text{H-S} \quad n=3,4,\dots$	$k_{8E}$ $k_{8,n}$

RDS, rate determining step.

The finished kinetic model is developed by use of these elementary steps with some assumptions. The rate determining steps for the process are No. (1),(7) and (8). Steady state concentration are assumed for all surface intermediates. One of the major assumptions in the model is the desorption rate of alkenes,

which corresponds to elementary step No. 8. These assumptions among others were made to establish the final model. Description of chain growth probabilities are dependent on increasing carbon number and are given by:

$$\alpha_1 = \frac{k_3 K_1 P_{\text{CO}}}{k_3 K_1 P_{\text{CO}} + k_{7\text{M}} \sqrt{K_2 P_{\text{H}_2}}} \quad (3.1)$$

$$\alpha_2 = \frac{k_3 K_1 P_{\text{CO}} [S]}{k_3 K_1 P_{\text{CO}} [S] + k_7 \sqrt{K_2 P_{\text{H}_2}} [S] + K_{8,\text{E}} e^{c \cdot 2}} \quad (3.2)$$

$$\alpha_n = \frac{k_3 K_1 P_{\text{CO}} [S]}{k_3 K_1 P_{\text{CO}} [S] + k_7 \sqrt{K_2 P_{\text{H}_2}} [S] + K_{8,0} e^{c \cdot n}} \quad n \geq 3 \quad (3.3)$$

The constant  $c$  expresses weak Van der Waals forces between the chain and the surface of each of the C-atoms. With a value of -0.27 the model matched with literature values for cobalt F-T catalyst. Reaction rate constants  $k_i$  could be calculated according to the arrhenius equation with temperature as the only variable, see Equation 3.4. Equilibrium constants (K) are calculated by assuming no change in entropy, as given by Equation 3.5.[12]

$$k = A \times e^{-E/RT} \quad (3.4)$$

$$K = A \times e^{-\Delta H/RT} \quad (3.5)$$

The expression for describing [S] found by Todic et al.[2] were found to be incorrect. After contacting the authors the expression was corrected to:

$$[S] = 1 / (1 + K_1 P_{\text{CO}} + \sqrt{K_2 P_{\text{H}_2}} + (\frac{1}{K_2^2 K_4 K_5 K_6} \frac{P_{\text{H}_2\text{O}}}{P_{\text{H}_2}^2} + \sqrt{K_2 P_{\text{H}_2}}) \cdot (\alpha_1 + \alpha_1 \alpha_2 + \alpha_1 \alpha_2) (\sum \prod \alpha_j)) \quad (3.6)$$

Equation 3.6 is an implicit non-linear function of a single variable S, which has to be solved in the range between 0-1. The production rates for C<sub>1</sub>-C<sub>15</sub> alkenes and C<sub>2</sub>-C<sub>15</sub> alkenes are given by:

$$R_{\text{CH}_4} = k_{7\text{M}} K_2^{0.5} P_{\text{H}_2} \alpha_1 \cdot [S]^2 \quad (3.7)$$

$$R_{C_n H_{2n+2}} = k_7 K_2^{0.5} P_{H_2}^{0.5} \alpha_1 \alpha_2 \prod \alpha_i \cdot [S]^2 \quad n \geq 2 \quad (3.8)$$

$$R_{C_2 H_4} = k_{8E,0} e^{c \cdot 2} \alpha_1 \alpha_2 [S] \quad (3.9)$$

$$R_{C_n H_{2n}} = k_{8,0} e^{c \cdot n} \alpha_1 \alpha_2 \prod \alpha_i [S] \quad n \geq 3 \quad (3.10)$$

### 3.1 Model Implementation

The present section includes the different steps for implementing the explained kinetic model is included. Firstly, a verification of the results, by use of MATLAB, is needed. When the production rates are confirmed to be similar with the article, implementation in HYSYS will commence.

#### Verification of the kinetic model

Todic et al. [2] used collected data from a stirred tank slurry experiment to define the needed kinetic parameters for their model. The parameters and estimated values of the model are presented in Table 3.2. All reaction rates ( $k_i$ ) and equilibrium constants ( $K_i$ ) are calculated from these values. The whole model was then implemented in MATLAB to verify the calculated results in the article. All relevant kinetic scripts regarding this implementation are included in Appendix A. The model uses a probability value ( $\alpha$ ) that changes with increasing carbon number, see Figure 3.2. The production rates for C<sub>2</sub>-C<sub>15</sub> alkanes and C<sub>2</sub>-C<sub>15</sub> alkenes are presented in Figure 3.3.

The MATLAB script proved to give similar results as Todici et al. [2] achieved with similar process conditions. This confirms right implementation of the model which allows the implementation into HYSYS Version 8.0 to begin.

#### HYSYS implementation

Aspen HYSYS software has made it possible to add custom objects into their simulation environment. This is included to enhance the functionality of the software when the included functionalities are not sufficient for a process simulation. The custom object to include in this project are the description of production rate for alkanes and alkenes given by Todici et al.[2].

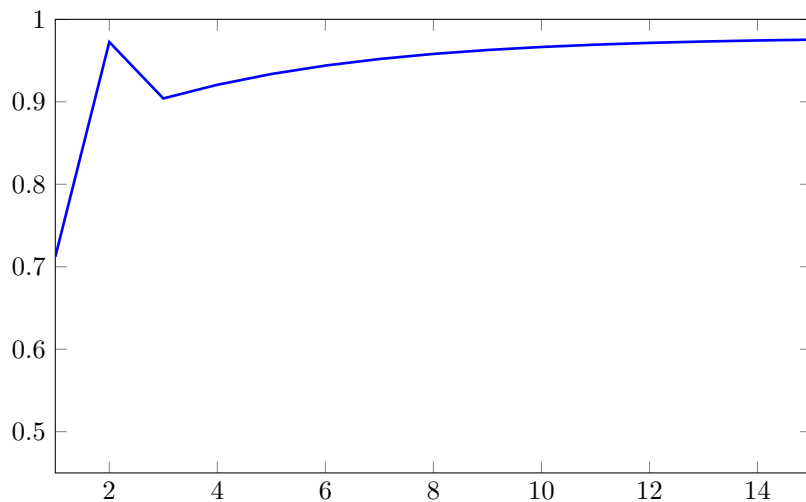


Figure 3.2: Chain growth probability ( $\alpha_n$ ) plotted against increasing carbon number. Calculated from the MATLAB script presented in Appendix A.

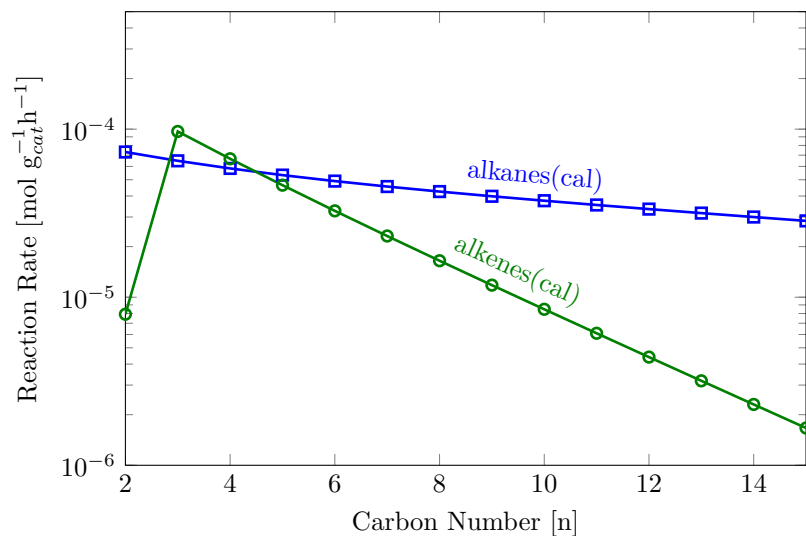


Figure 3.3: Calculated production rates for alkanes and alkenes at  $T=200$  [°C],  $P=1.5$  [MPa],  $H_2/CO = 2.1$  using the MATLAB script presented in Appendix A.

Table 3.2: All kinetic parameters that was used to calculate the given reaction rates and equilibrium constants for the Todici et al.[2] kinetic model

Parameter	Value	Unit	Parameter	Value	Unit
$A_1$	$6.59 \times 10^{-5}$	[MPa <sup>-1</sup> ]	$\Delta H_1$	-48.9	[kJ/mol]
$A_2$	$1.64 \times 10^{-4}$	[MPa <sup>-1</sup> ]	$\Delta H_2$	-9.4	[kJ/mol]
$A_3$	$4.14 \times 10^8$	[mol g <sub>cat</sub> <sup>-1</sup> h <sup>-1</sup> ]	$E_3$	92.8	[kJ/mol]
$A_4$	$3.59 \times 10^5$	-	$\Delta H_4$	16.2	[kJ/mol]
$A_5$	$9.81 \times 10^{-2}$	-	$\Delta H_5$	11.9	[kJ/mol]
$A_6$	$1.59 \times 10^6$	[MPa]	$\Delta H_6$	14.5	[kJ/mol]
$A_7$	$4.53 \times 10^7$	[mol g <sub>cat</sub> <sup>-1</sup> h <sup>-1</sup> ]	$E_7$	75.5	[kJ/mol]
$A_8$	$4.11 \times 10^8$	[mol g <sub>cat</sub> <sup>-1</sup> h <sup>-1</sup> ]	$E_8$	100.4	[kJ/mol]
$A_{7M}$	$7.35 \times 10^7$	[mol g <sub>cat</sub> <sup>-1</sup> h <sup>-1</sup> ]	$E_{7M}$	65.4	[kJ/mol]
$A_{8E}$	$4.60 \times 10^7$	[mol g <sub>cat</sub> <sup>-1</sup> h <sup>-1</sup> ]	$E_{8E}$	103.2	[kJ/mol]

HYSYS software requires each of the reactions to be implemented separately as a Kinetic Reaction Extension. This resulted in 29 extensions describing the production rates for C<sub>1</sub>-C<sub>15</sub> alkanes and C<sub>2</sub>-C<sub>15</sub> alkenes. HYSYS uses two separate files for each of the extensions to work properly: Dynamic Link Library (DLL) File and Extension Definition File (EDF). The DLL file is created with the use of Microsoft Visual Basic 6 where the extension code is included. There are two main subroutines in this code, Initialize and Reaction Rate. The Initialize routine is only called one time whenever the extension is first added to the software. Parameters like the stoichiometric coefficients and base components are included in this subroutine. Reaction rate subroutine runs when the extension is used in a simulation case. This calculates the consumption rate of a specified base component and returns the value back to HYSYS. The EDF file is created by View Editor which is included in the process simulator program UniSim Design R400 and contains the needed definitions of the extension. This EDF file works as the link between the created extension code and HYSYS, see Figure 3.4.

The necessary DLL and EDF files were created and separately registered into Aspen HYSYS software. Each of the extensions were then tested at various process conditions and compared with MATLAB results. As an example the DLL Extension code written in Visual Basic 6 for pentene is included in Appendix B. Reaction rate results from HYSYS were then compared with the similar results in MATLAB. All of the values is presented in Table 3.3.

The results clearly show similar production rates for pentene at different process conditions which indicates correct implementation of the given kinetic model. Similar tests was also conducted for the 28 remaining extensions with similar

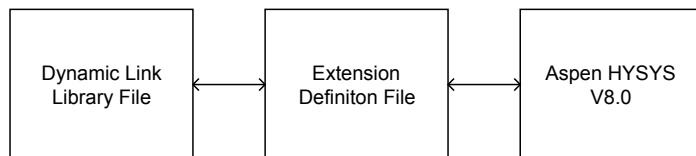


Figure 3.4: An illustration on how the extension code is sent to the AspenTech HYSYS V8.0 software. The EDF file is the link between the extension code and the software.

Table 3.3: Reaction rate comparison test for MATLAB and HYSYS at six different process conditions.

Conditions $P[\text{MPa}]$ $T[^\circ\text{C}]$	Reaction Rate <b>MATLAB</b> $[\text{mol g}_{cat}^{-1}\text{h}^{-1}]$	Reaction Rate <b>HYSYS</b> $[\text{mol g}_{cat}^{-1}\text{h}^{-1}]$
$P_{\text{H}_2}=0.75$ $P_{\text{CO}}=0.25$ $T=172.15$	$1.63 \cdot 10^{-05}$	$1.63 \cdot 10^{-05}$
$P_{\text{H}_2}=0.25$ $P_{\text{CO}}=0.75$ $T=172.15$	$1.22 \cdot 10^{-05}$	$1.22 \cdot 10^{-05}$
$P_{\text{H}_2}=0.75$ $P_{\text{CO}}=0.25$ $T=200.15$	$1.18 \cdot 10^{-04}$	$1.18 \cdot 10^{-04}$
$P_{\text{H}_2}=0.25$ $P_{\text{CO}}=0.75$ $T=200.15$	$1.11 \cdot 10^{-04}$	$1.10 \cdot 10^{-04}$
$P_{\text{H}_2}=0.75$ $P_{\text{CO}}=0.25$ $T=222.15$	$4.36 \cdot 10^{-04}$	$4.40 \cdot 10^{-04}$
$P_{\text{H}_2}=0.25$ $P_{\text{CO}}=0.75$ $T=222.15$	$4.99 \cdot 10^{-04}$	$5.02 \cdot 10^{-04}$

results. The specific values for each of the rates are included in Appendix C.

## 3.2 Model Limitations

The implemented model have only included the production of hydrocarbons up to  $\text{C}_{15}$  even though products up to  $\text{C}_{30}$  and higher are produced.[3] The reason for this limitation is due to how the extensions are included in the Aspen HYSYS software. Each of the reactions have to access their own DLL and EDF file, causing the simulation time to increase significantly when more reactions are added. This effect made it both difficult and tedious to include more than 29 products. It is expected that the consumption of CO would increase when more

reactions are included. This was tested by using the implemented MATLAB script described in the previous subsection. The result indicated that a product increase from  $C_{15}$  to  $C_{30}$  would increase the CO consumption by roughly 80 %. This limitation is crucial to remember when the results are being evaluated since the overall response would change significantly if more products were included.



# Chapter 4

## Simulation Model

The Gas-to-Liquid plant was simulated using Aspen process simulator HYSYS Version 8.0. Peng-Robinson was selected as the property package for this simulation because it has an accurate equilibrium calculation for systems consisting of mainly hydrocarbons.

There are three different configuration designs that will be simulated: the Base Case, Configuration 1 and 2. The differences between them are presented in this chapter. All assumptions and design parameters for these configurations was determined in collaboration with my main supervisor, prof. Magne Hillestad.[13]

### 4.1 Base Case Configuration

This simulation uses a conventional GTL design which converts natural gas into the desired products, namely liquid hydrocarbon (wax). A modern hydrogen plant process is also included in the process due to the need for pure hydrogen in the upgrading unit. The configuration layout for this process is included in Figure 2.1.

### GTL Plant

The feedstock for the simulation is natural gas consisting of mainly methane. Molar fractions for this stream are specified in Table 4.1.

Table 4.1: The feedstock for the different simulations: Natural gas with its related mol fractions.

Compostion	Mol fractions
Methane	0.95
Ethane	0.02
Propane	0.015
i-Butane	0.01
i-Pentane	0.005

Natural gas enters the system at 50°C and 15 bar. It is then preheated to 400°C by a fired heater before entering the pre-reformer together with steam. In this step small amounts of higher hydrocarbons present in the natural gas are converted into methane. The product is then preheated to 500°C before being mixed with pure oxygen into the ATR. The amount of steam into the reformer is adjusted until the H<sub>2</sub>/CO ratio is roughly 2, while the O<sub>2</sub> would be adjusted until 1000°C out of the ATR is reached. After that synthesis gas is produced, water is separated by cooling the stream down to 30°C. Synthesis gas is then preheated to 210°C before entering the Fischer-Tropsch reactor. This reactor is a multitube PFR with catalyst pellets inside the tubes. The reactor and catalyst specifications are given in Table 4.2.

Table 4.2: The main specifications of the Fischer-Tropsch reactor regarding overall design, cooling and choice of catalyst size.

	Parameter	Value	Unit
<b>Design</b>	Tube length	12	[m]
	Number of tubes	67500	
	Tube Diameter	0.025	[m]
	Wall thickness	0.005	[m]
	Total tube volume	400	m <sup>3</sup>
<b>Cooling</b>	Heat transfer coefficient	2000	[W m <sup>-2</sup> °C <sup>-1</sup> ]
	Mole flow	1·10 <sup>21</sup>	[kmol h <sup>-1</sup> ]
	Heat capacity	75	[kJ kmol <sup>-1</sup> °C <sup>-1</sup> ]
	Inlet temperature	250	[°C]
<b>Catalyst</b>	Particle diameter	0.01	[m]
	Solid density	1010	[kg m <sup>-3</sup> ]
	Void fraction	0.450	

The selected cooling medium for the F-T reactor is 250°C boiling water. A large amount of this flow is used to have no temperature increase in the cooling medium throughout the reactor. The energy output from this reactor would be used for the production of high pressure steam. An additional steam amount would be added if more high pressure steam is needed in the system. The reaction set in the reactor is the implemented kinetic model explained in Chapter 3. The products leaving the multitube PFR is then cooled down to 30°C and separated into three different phases: water, products ( $C_{5+}$ ) and unconverted reactants (gas).

## Hydrogen Plant

The main simulation design for the hydrogen plant is presented in Figure 2.3. Natural gas enters the system at 50°C and 15 bar before being preheated to 400°C. This preheating is achieved by utilizing heat from the resulting fuel tail gas in the steam reformer. After this step the natural gas is introduced into the pre-reformer together with steam. The steam amount is adjusted until a steam/carbon mole ratio of 3 is reached. Higher hydrocarbons are then reformed to mainly methane, before the process amount is heated to 650°C when entering the primary reformer, namely SMR. It is required to add energy into this reformer due to the endothermic reaction taking place (Reaction 2.2a). This energy amount is adjusted until the outlet temperature of 850°C is reached. The stream is then cooled down to 370°C as it is entering the high temperature shift converter. This step converts the remaining CO and water into Hydrogen and CO<sub>2</sub> according to Reaction 2.2b. Now the remaining part will be to separate the produced hydrogen from other products. This is achieved by use of pressure swing adsorber as described in Section 2.6. In the simulation environment this unit would be implemented as a component splitter where the hydrogen stream has a purity of 99.9 %.

The hydrogen production for the Base Case is going to be set at a fixed value. This amount will account for the excess hydrogen needed in an upgrading unit in a gas-to-liquid plant.

## 4.2 Configuration 1

The main idea for this configuration is to replace some of the required steam amount into the synthesis gas production with CO<sub>2</sub>. This amount of CO<sub>2</sub> is produced as a waste product in the hydrogen plant and is desirable to utilize for increasing the overall carbon efficiency of the system. This implementation will

make it possible to make synthesis gas with lower  $H_2/CO$  ratio but also reduce the amount of excess steam into the process, which is highly beneficial for wax production. The process configuration which will be simulated is presented in Figure 4.1.

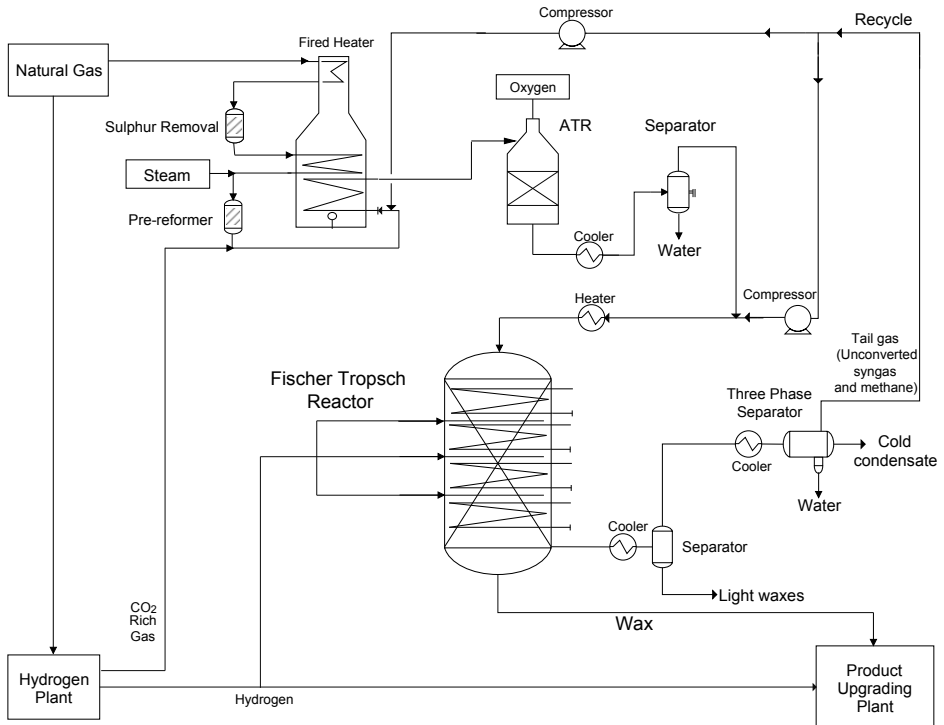


Figure 4.1: The first of two new GTL-configurations that will be simulated: Configuration 1. A  $CO_2$  rich tail gas from the hydrogen plant will be utilized for synthesis gas production. It will also be distributed along the PFR reactor to adjust the  $H_2/CO$  ratio to a desired value.

Hydrogen will be distributed along the reactor to maintain the consumption of hydrogen. The amount will be adjusted separately to maintain an equal  $H_2/CO$  ratio between each stages. This is included in order to reduce the degree of freedom in the system to get a better overall understanding of how the kinetic responds to different  $H_2/CO$  ratios. The design parameters like temperatures, catalyst bulk density, reactor size etc. will be held similar as in the Base Case

Configuration. The main difference between the cases is how natural gas is distributed. It can either be sent to the synthesis gas production or the hydrogen plant. The flow rate of natural gas into the system ( $F_0$ ) will be held constant for all of the configurations. In this way equal amounts of carbons are injected into the system and simulation results can be compared with each other.

### 4.3 Configuration 2

This configuration is similar to the previous one in that  $\text{CO}_2$  replaces some of the steam used in the synthesis gas production and an equal amount of  $F_0$  is being processed. One major difference is the F-T reactor design. In the two previous simulations there have only been one single PFR. This is now divided into three smaller reactors keeping the total volume the same. Between reactors both water and products ( $\text{C}_{5+}$ ) are removed by use of a horizontal three phase separator. A stream of pure hydrogen is then injected between each of the reactors to adjust the  $\text{H}_2/\text{CO}$  ratio to the desirable value. The process configuration that will be simulated is presented in Figure 4.2.

Cost evaluation regarding this configuration is also evaluated. In Configuration 1 there is no need to invest in any additionally process equipment when comparing it with the Base Case Configuration. This is however not the case for Configuration 2. It is needed to buy two additional three phase separators, two coolers, and two heaters for this configuration to be operational.

### 4.4 Heat Integration

One major improvement regarding the overall energy efficiency of the system is to utilize heat present in hot streams to heat up streams at lower temperatures. The theory related to this subject is presented in section 2.7.

The chosen hot streams that would be used for heat utilization are:

1. Auto Thermal Reformer Outlet (Synthesis Gas Production.)
2. Fischer-Tropsch Outlet
3. Steam Reformer Outlet (Hydrogen Production)
4. Water Gas Shift Outlet (Hydrogen Production)

The process stream out of the ATR is selected to be the main source for production of electrical power. The energy in this stream would be introduced in

a waste-heat boiler (WHB) where high pressure steam is formed. This amount would undergo an expansion in a suitable turbine where electrical energy is generated. Stream 1 will be used for heat utilization if no other stream are available. Cold streams that are desirable to heat up are:

5. Pre-reformer Outlet (Synthesis Gas Production)
6. Fischer-Tropsch Inlet
7. Pre-reformer Outlet (Hydrogen Production)
8. Natural Gas Inlet (Synthesis gas production)

It is assumed that the needed energy to heat up natural gas that enters the hydrogen plant are fulfilled by exploiting energy present in the tail gas produced in the steam methane reformer. This is why this stream is not included into the heat integration. Stream 5 uses a natural gas driven fired heater to reach its desirable temperature. It would be beneficial for the configuration if this heater could be removed or even been reduced in size. Smaller FHR would reduce investment cost but also the operational cost since less fuel is used.

A heat integration analysis will be evaluated for both the Base Case and the new configuration that gives most promising result regarding energy efficiency.

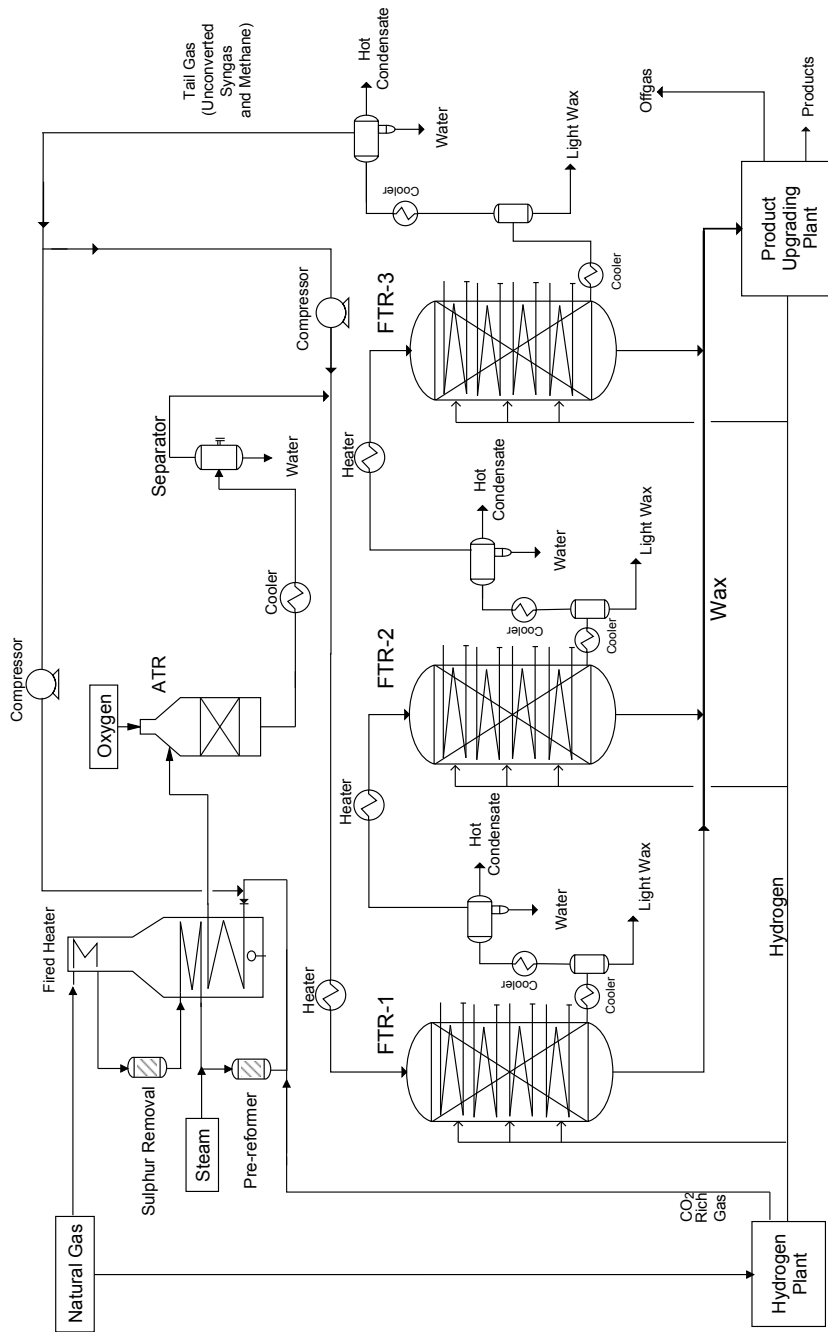


Figure 4.2: The second new GTL-configuration where one large reactor have been divided into three smaller ones: Configuration 2. Both water and products are separated between each of the reactors to improve the overall efficiency.





# Chapter 5

## Results and Discussion

The simulations were constructed as explained in Chapter 4. All results were generated using kinetics from Todic et al.[2] with temperature, pressure and composition dependent  $\alpha$  value.

One important comment about this analysis is that all of the simulations are conducted with one pass through the reactor. In an actual plant a recycle stream would be included since this would convert unconverted reactants and improve the overall efficiency significantly. This was however impossible to include due to the model implementation presented in Section 3.2. It was therefore decided that the flow into the system would be adjusted until 80 % of conversion of CO in the PFR was reached. The thermal efficiency for combustion was also assumed to be 80 %.

### 5.1 Base Case Configuration

The Base Case Configuration was simulated as described in Section 4.1. It was assumed that the given Fischer Tropsch reactor (PFR) should reach a conversion of 80 % per pass through the reactor. In order to reach this conversion the amount of natural gas into the system was set to be 22000 kmol/h. In this case all of the natural gas was processed in the synthesis gas production while hydrogen production will be evaluated later.

The first major simulation unit was the ATR. This unit would convert methane to synthesis gas. There was used a Gibbs reactor to resemble this unit. A response

test was conducted to conform correct response from this simulation. Results from this analysis is presented in Table 5.1.

Table 5.1:  $H_2/CO$  ratio and temperature response out of the ATR when increasing each of the inlet streams individually.

Parameter	$H_2/CO_{Out}$	$T_{Out}$
$O_2$ Ammount $\uparrow$	$\downarrow$	$\uparrow$
$H_2O$ Ammount $\uparrow$	$\uparrow$	$\downarrow$
Natural Gas Ammount $\uparrow$	$\uparrow$	$\downarrow$

More oxidation reactions occur when higher amounts of  $O_2$  is introduced into the reactor. This resulted in a synthesis gas with lower  $H_2/CO$  ratios while the temperature out of the reactor increased. Opposite effect is noticed when steam and natural gas amount are increased separately. This is because more endothermic reactions are occurring in the reactor. The response from the simulation corresponds well with the main reactions occurring in this unit. These reactions are presented at page 7.

Synthesis gas for Fischer Tropsch processing should have a  $H_2/CO$  ratio of roughly 2. Therefore, it was required to use 11 000 kmol/h of steam into the reactor to fulfil this requirement. The amount of oxygen was adjusted 1000°C was reached. These inlet flows gave a synthesis gas with a  $H_2/CO$  ratio of 2.13 which was considered to be acceptable for further processing in the Fischer Tropsch. Final amounts and properties entering the process are presented in Table 5.2.

Table 5.2: Final amount and process conditions for the three inlet flows in the Base Case Configuration: Natural gas, Oxygen and Steam.

Property	Natural Gas	$O_2$	Steam
Pressure [Bar]	15	15	15
Temp [°C]	50	20	199
Flow rate [kmol h <sup>-1</sup> ]	22000	13000	11000
Mass Flow [kg h <sup>-1</sup> ]	384000	42000	198000

The synthesis gas was sent to the multitubular PFR after water removal and preheating. This reactor used the kinetic model by Todić et al. [2] for describing the product distribution of both alkanes and alkenes. The resulting temperature profile in this PFR reactor is presented in Figure 5.1.

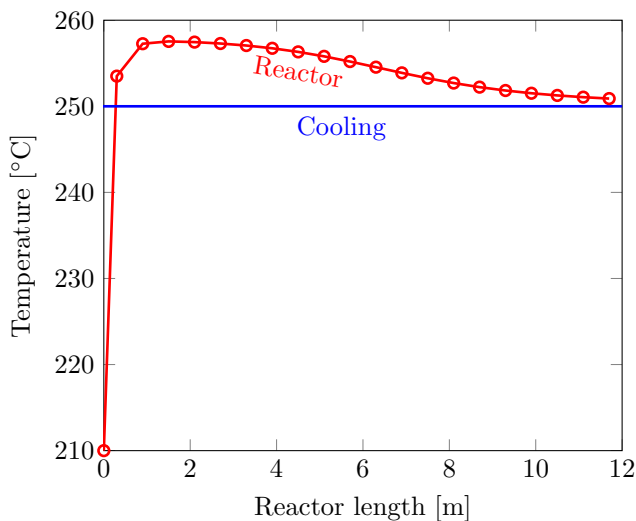


Figure 5.1: The resulting temperature profile along the 12 meter long PFR reactor in the Base Case Configuration.

A rapid temperature increase in the reactor was expected due to the highly exothermic reactions occurring in the reactor. The temperature eventually stabilized at 250°C when most of the synthesis gas had reacted. The importance of heat removal in this reactor proved to be high. The produced energy had to be removed fast and efficiently for the desired reactions to occur properly. Composition and weight fractions along the 12 meter long PFR reactor are presented in Figure 5.2 and 5.3.

The reactor outlet stream then undergoes stepwise separation to separate the products. The different production amounts are presented in Table 5.3.

It is clear that the production of alkanes are considerable higher than alkenes. A response test of the Fischer-Tropsch process was executed to discover which variables had a small or large effect on the main parameters like conversion per pass, methane and  $C_{5+}$  production. Results from increasing each of the variables by 20% is presented in Table 5.4.

When decreasing the same variables by 20% the opposite effect was noticed. This indicates that lower  $H_2/CO$  ratio favors the production of longer hydrocarbon chains ( $C_{5+}$ ) while methane production is less favourable. These two responses are the desired effect for an optimal design: To have the highest possible production of longer chains while minimizing the production of methane. Higher

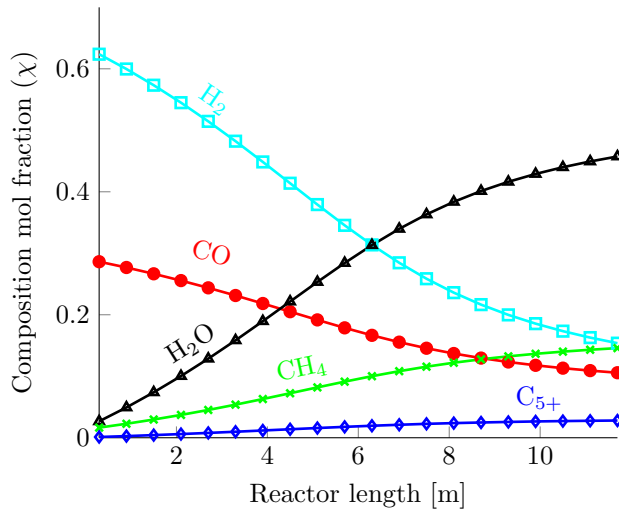


Figure 5.2: A plot displaying the main component mol fractions changes along the 12 meter long PFR reactor. The result is collected from the Base Case Configuration.

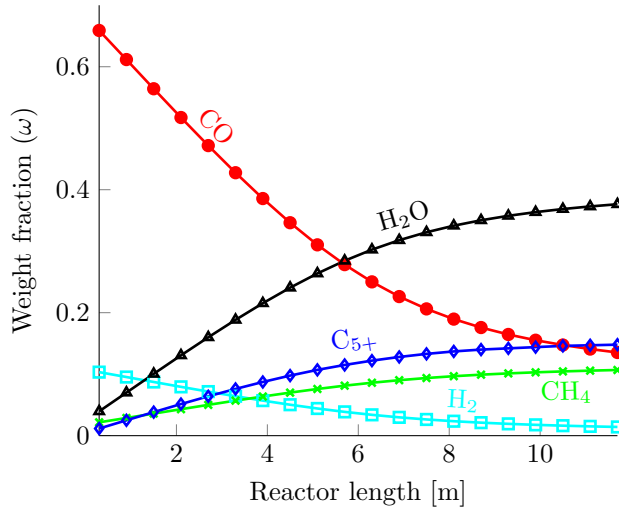


Figure 5.3: A plot displaying the weight fraction changes through the 12 meter long PFR reactor. All the data is gathered from the Base Case Configuration.

Table 5.3: The final production amounts in the Base Case Configuration. This included both alkanes and alkenes, C<sub>1</sub> to C<sub>15</sub>.

Component	Alkanes	Alkenes	Alkanes	Alkenes
	[kmol/h]	[kmol/h]	[kg/h]	[kg/h]
C <sub>1</sub>	5441	x	87000	x
C <sub>2</sub>	253	29	7600	800
C <sub>3</sub>	196	281	8600	12000
C <sub>4</sub>	157	170	9100	9500
C <sub>5</sub>	129	106	9300	7400
C <sub>6</sub>	108	67	9300	5600
C <sub>7</sub>	92	43	9200	4300
C <sub>8</sub>	79	28	9000	3200
C <sub>9</sub>	69	19	8800	2400
C <sub>10</sub>	60	13	8600	1800
C <sub>11</sub>	53	8	8300	1300
C <sub>12</sub>	47	6	8000	900
C <sub>13</sub>	41	4	7700	700
C <sub>14</sub>	37	3	7300	500
C <sub>15</sub>	33	2	7000	400

Table 5.4: The kinetic response for the Fischer-Tropsch synthesis when increasing the H<sub>2</sub>/CO ratio in the synthesis inlet, pressure and total tube reactor volume individually.

Parameter 20 % Increase	Conversion per pass	Methane prod.	C <sub>5+</sub> prod.
<i>H<sub>2</sub>/CO Ratio</i> ( Syngas Inlet)	↑	↑	↓
<i>Pressure</i> [bar]	↑	(↓)	↑
<i>Reactor Volume</i> [m <sup>3</sup> ]	↑	↑	↑

pressure and larger reactor volume increased conversion per pass resulting in higher production of both methane and C<sub>5+</sub> which was anticipated. The next subsection includes results related to the production of pure hydrogen.

## Hydrogen Plant

The hydrogen plant was simulated as described in Section 4.1. The process configuration produced 10 000 kmol/h of 99.9 % pure hydrogen from 3500 kmol/h of natural gas. There was additionally produced a tail gas amount from this plant. This consist of different components, see Table 5.5.

Table 5.5: The final pressure swing absorber (PSA) tail gas composition.

Component	Mol fractions
H <sub>2</sub> O	0.45
CO <sub>2</sub>	0.24
H <sub>2</sub>	0.18
CO	0.08
CH <sub>4</sub>	0.05
TOTAL	1.00

There are amounts of carbon present in both CO<sub>2</sub> and CH<sub>4</sub> which would be desirable to utilize for improving the overall efficiency of the system. This is where the two new configurations are being introduced. They utilize this tail gas for synthesis gas production which will alter the overall response of the system. The results from these two new configurations will be compared with the Base Case Configuration results to evaluate which of the configurations are the most beneficial for the production of higher hydrocarbon chains (C<sub>5+</sub>). All results regarding this analysis are presented in the following section.

## 5.2 Main Analysis

The two new gas-to-liquid configuration was first simulated according to the specifications given in Chapter 4. The total amount of used natural gas ( $F_0$ ) that could end up as final products was kept constant at 22 000 kmol/h for all of the three configurations. The amount of hydrogen that will be sent to the product upgrading will be held constant for all of the configurations. These two measures needs to be fulfilled for the results to be comparable.

The synthesis gas H<sub>2</sub>/CO ratio was the main parameter that was adjusted between the different configurations. In the Base Case Configuration a synthesis gas with a ratio of 2.2 was produced. When the tail gas amount was introduced in Configuration 1 and 2, the ratio was decreased to 1.6. Configuration 1 and 2

are distributing pure hydrogen between each of the stages/reactors. This is to maintain the consumption of hydrogen along the reactor length. The H<sub>2</sub>/CO adjustment was set to be similar as the ATR outlet, namely 1.6. This was decided to limit the many degrees of freedom in the process. The resulting temperature profile and how H<sub>2</sub>/CO ratio changes through the reactor in Configuration 1 is presented in Figure 5.4.

All of the main results for each of the configurations are presented in Table 5.6. Each of the different parameters will in the continuing subsection be discussed separately. The intention of presenting it in this way was to highlight the most important results in a effective and understandable manner.

Table 5.6: Main results comparison for the different configurations: Base Case, Configuration 1 and 2

Parameter		Base Case	Config. 1	Config. 2
Product mass flow (C <sub>5+</sub> )	[barrels/day]	23 000	23 500	30 000
	[kg/h]	104 000	107 000	134 500
Molar C <sub>5+</sub> Difference	[%]	0	-0.2	18
Carbon Efficiency	[%]	23	25	31
(C <sub>Prod</sub> / C <sub>Feed</sub> + C <sub>Fuel</sub> )				
Energy Efficiency	[%]	7	11	13
(E <sub>Prod</sub> / E <sub>Feed</sub> + Q)				
Methane Difference	[%]	0	-27	-20
CO Conversion Per Pass PFR	[%]	80	76	88
Unconverted CO	[kmol/h]	3 950	4 600	2 250
H <sub>2</sub> /CO ratio after ATR		2.2	1.6	1.6

## Mass flow of products

The main objective with the project was to find a GTL-configuration that favors the production of longer hydrocarbon chains (C<sub>5+</sub>). Configuration 2 shows a large increase in product mass flow compared to the Base Case Configuration and Configuration 1. This increase is explained by a change in residence time. Configuration 2 uses three smaller reactors instead of one large. Water and products are being separated between each of these reactors. The total reactor volume is the same for all the configurations but by removing these streams an increase in residence time occurs. Higher residence time will increase the conversion of reactants (CO+H<sub>2</sub>) resulting in higher production amounts.

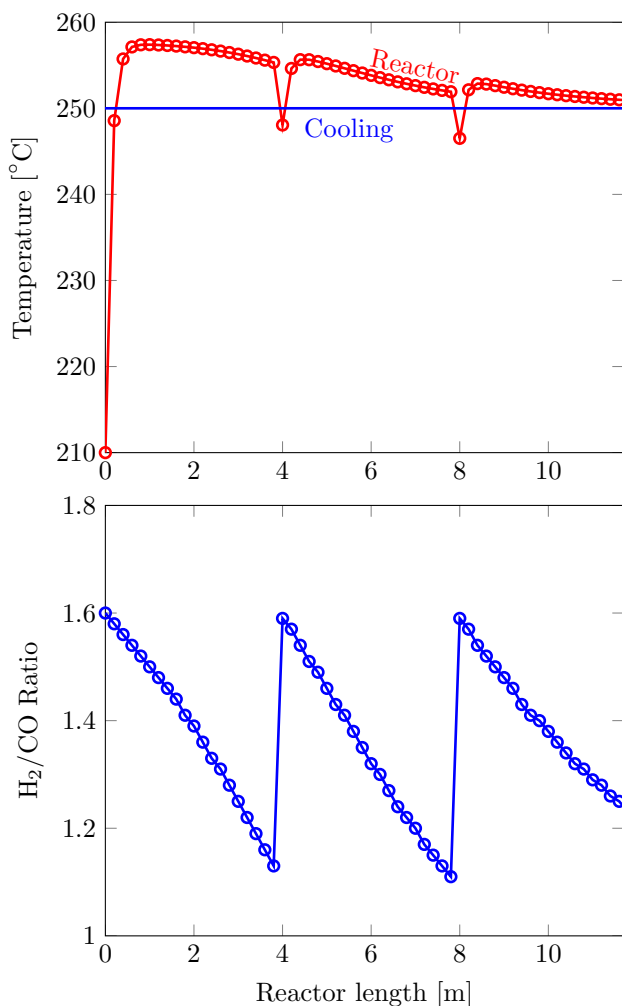


Figure 5.4: The resulting temperature profile along the 12 meter long PFR reactor, Configuration 1. It is also included how the  $H_2/CO$  ratio was adjusted with pure hydrogen to a level of 1.6 along the reactor length.

One interesting effect to discuss is how the products ( $C_5 - C_{15}$ ) are distributed in each of the configurations. This is presented in Table 5.7.

The total molar sum of alkanes and alkenes are almost similar for the Base Case



Table 5.7: The product distribution for each of the configurations: Base Case, Configuration 1 and 2. This included the mol flows for alkanes, alkenes and the total amount.

Mol SUM of:	Base Case	Config. 1	Config. 2
Alkanes [kmol/h]	749	704	839
Alkenes [kmol/h]	298	341	395
TOTAL [kmol/h]	1046	1045	1233

and Configuration 1 while the distribution between them has changed. Configuration 1 processes a synthesis gas with a lower  $H_2/CO$  ratio than the Base Case Configuration, 1.6 against 2.2. The response from this is a decrease in alkane production while the alkene production increases. This indicates that processing a synthesis gas with a lower  $H_2/CO$  ratio would not increase production amounts by itself. Configuration 2 shows that a different reactor design have a larger impact regarding production amounts since higher amounts of alkanes and alkenes are being produced.

## Carbon Efficiency

Carbon efficiency is defined as the number of carbons present in products divided by the number of carbons entering the system. All of the different configurations uses natural gas as fuel for combustion in both fire heaters (FH) and in the SMR unit (hydrogen plant). These natural gas amounts were all included to give a realistic result regarding carbon efficiency. The highest carbon efficiency for one pass through the reactor was achieved with Configuration 2. This efficiency corresponded to 31 %. This was achieved mainly of the different reactor design used in this configuration. Three smaller reactor stages with water and products separation gave an increase in residence time and thus increased the efficiency. One other contribution that increased the carbon efficiency was the utilization of tail gas from the hydrogen plant for synthesis gas production. Carbon present in this amount was in this way being converted into products instead of being emitted as pollution.

## Energy Efficiency

Energy efficiency is defined as energy leaving in the products streams ( $C_{5+}$  and hydrogen) divided by the external energy input ( $Q$ ) together with energy entering in the inlet streams. The high pressure steam production from the Fischer-Tropsch reactor provided the steam requirement for the systems. This leaves the inlet streams to be natural gas and oxygen. Natural gas however was being used in three different places: synthesis gas production, hydrogen plant and furnaces (FH and SR). The energy present in each of the process inlet streams was obtained by heat flows presented in the AspenTech HYSYS simulation. An external input of energy ( $Q$ ) was needed to be included for the process configuration to be functional. The natural gas from the pre-reformer in the synthesis gas production needed additional heating before it could enter the ATR. Similar preheating was needed in the hydrogen plant, between the pre-reformer and steam reformer. It is also required to preheat the synthesis gas after water removal to 210 °C before entering the PFR. There were two extra energy inputs needed in Configuration 2 because of water and product separation between each of the reactors.

Despite this additional energy input, Configuration 2 proved to give the highest energy efficiency, namely 13 %. The reason why this level was so low is mainly due to the fact that it was only possible to simulate one pass through the PFR reactor. If a recycle stream would have been introduced a higher efficiency would be expected. One way to increase the energy efficiency is to decrease the external energy input ( $Q$ ) into the system. A detailed analysis of this approach is presented in Section 5.3.

## Methane production

An optimal gas-to-liquid configuration would favor production of longer hydrocarbon chains but also produce small amounts of methane. The less synthesis gas being converted to methane the higher the efficiency and production amount would be.

Both Configuration 1 and 2 gave a reduction in methane production compared to the Base Case, respectively 26.6 % and 20.2 %. This enhance of performance, as compared with the Base Case, is mainly due to processing a synthesis with lower  $H_2/CO$  ratio. There will be a lower probability for the hydrocarbon chains to terminate if less hydrogen is present in the process stream. Changing the synthesis gas  $H_2/CO$  ratio parameter by itself makes a large difference in methane selectivity. This result have to be included when other process configurations and conditions are being evaluated to find an optimal GTL-configuration.

## CO conversion per pass in PFR

One other parameter that changes between the configurations are the conversion per pass. Decreasing  $H_2/CO$  ratio in the synthesis reduces the conversion per pass in the F-T reactor slightly. This results in more unconverted CO in configuration 1 then the base case configuration. Increasing recycle amounts or reactor volume would eliminate this difference. The largest conversion is achieved with Configuration 2 which conforms the previous discussion about higher residence time.

This was the last parameters in Table 5.6 that will be discussed. The next subsection discusses the flow distribution between each of the different configurations.

## Flow Distribution

An optimal GTL-configuration could not be determined only by considering which design gives the highest carbon efficiency. The necessary inlet flows for each of the different configurations need also to be evaluated. A configuration that reduces the overall usage of external steam or oxygen is also highly desirable. An overview for the main process amount for each of the configurations are therefore included in Table 5.8. The flow amounts are rounded to the closest five hundred value for the sake of simplicity.

The amount of natural gas that could be converted to products ( $F_0$ ) are equal for three configurations cases, 22 000 kmol/h. The distribution of  $F_0$  is highly different for the configurations. For the Base Case all of the  $F_0$  is processed in the synthesis gas production while the two other configurations process some of the amount in the hydrogen plant. Additionally there is sent a separate natural gas stream to hydrogen production of 3500 kmol/h. It is only included to produce roughly the same amounts of excess hydrogen for the upgrading unit as Configuration 1 and 2: 11 000 kmol. The tail gas that is produced from this hydrogen production is not being utilized in the synthesis gas production. This is the reason why the natural gas amount of 3500 kmol/h is not included into the  $F_0$  amount. The required amount of hydrogen which is needed to adjust the  $H_2/CO$  Ratio between each of the reactors/stages to a level of 1.6 is referred to as distributed hydrogen. This explains why there is no distribution of hydrogen in the Base Case.

The total steam consumption for the two new process configurations have increased by 12 % when comparing it with the Base Case. This increase is related to the steam to carbon requirements in the different production methods. There is a steam to carbon requirement of 0.5 in the synthesis gas production, while the

Table 5.8: Flow distributions for the different process configurations: Base Case, Configuration 1 and 2.

<b>Amount</b>	<b>Base Case</b> [kmol/h]	<b>Config. 1</b> [kmol/h]	<b>Config. 2</b> [kmol/h]
<b>Total amount NG into the system <math>F_0</math></b>	22000	22000	22000
Amount NG to synthesis gas production	22000	15000	15000
Amount NG to hydrogen production	(3500)	7000	7000
<b>Total hydrogen production</b>	11000	20500	20500
Distributed hydrogen	0	9000	10000
Excess hydrogen (Upgrading)	11000	11500	10500
<b>Total steam usage</b>	22000	24500	24500
Steam to synthesis gas production	11000	3500	3500
Steam to hydrogen production	10000	21000	21000
<b>Overall Oxygen Usage</b>	13000	10000	10000

same requirement for hydrogen production is 3. In Configuration 1 and 2 are 32 % of the  $F_0$  amount being processed in the hydrogen plant instead of synthesis gas. One effect that counteracts this increase is the utilization of tail gas produced in the hydrogen plant. This gas consist of a large amount of water and  $\text{CO}_2$  which makes it possible to reduce the amount of steam into the synthesis gas production for Configuration 1 and 2. This reduction is however still not possible to reduce to zero, due to the need for steam in the pre-reformer unit. It was therefore decided that 3500 kmol/h of steam into the pre-reformer step was the lowest value.

Another benefit from utilizing tail gas from the hydrogen plant is that the required oxygen demand for the two new configurations have been reduced, namely 23 %. This reduction is explained by evaluating the energy demand of converting one single carbon from  $\text{CH}_4$  to  $\text{CO}$ , see enthalpy requirements in reaction 2.2a and 2.2c at page 7. The needed energy for producing one  $\text{CO}$  molecule by the use of steam is 206 kJ/mol, the energy demand is 123.5 kJ/mol when  $\text{CO}_2$  is used. The amount of oxygen into the ATR is therefore reduced since the temperature requirement of the ATR ( $1000^\circ\text{C}$ ) is fulfilled earlier than for the Base Case. This results is highly interesting because this would make it possible to reduce the size of the air separation unit in configuration 1 and 2. This would result in a reduction in both investment and operational cost which would contribute to increasing the overall efficiency of a GTL-plant.

## Final Comments

The previous results have made it clear that Configuration 2 is the design which gives the most result regarding oxygen demand, carbon and energy efficiency. One thing that has to be mentioned for this configuration is the increase in investment cost. It is necessary to buy another two three phase separators, two coolers, and two heaters for the configuration to be functional. A rough cost calculation show that the additional investment cost would be significantly smaller less than the improvement regarding the mass flow of products.

A final note is that all of the simulations have been executed for one pass through the PFR reactor where only  $C_1$ - $C_{15}$  is produced. This simplification had to be done because of the limitation regarding implementation. If more products would have been included the product distribution would also be different. This simplification makes the project results to be more about the overall response rather than specific amounts and components. An example is included to emphasize this effect since this is crucial for the overall understanding of the project.

### Example: Configuration 2

It was discovered that Configuration 2 gave a large decrease in methane production while higher chains production increased. This result is the desired effect when evaluating a gas-to-liquid plant. The actual value of change would be different when more reactions are implemented, but the overall response is expected to be similar since an accurate kinetic model was used to describe of  $C_1$ - $C_{15}$  production.

## 5.3 Heat Integration

Because the levels of energy efficiency are low for all the configurations, it was therefore decided to conduct a heat integration analysis for the initial Base Case. The same would be done for Configuration 2 since this design gave the highest energy efficiency. All of the results regarding this analysis is presented in the subsequent subsections.

### 5.3.1 Base Case Configuration

The streams that were to be utilized in this heat integration are mentioned in section 4.4. There are in total four heat streams that are used to heat up four cold streams. The different temperature intervals and corresponding heat-capacity

flow rates for each of the streams are presented in Figure 5.5. All of the different values were found by using the AspenTech HYSYS software.

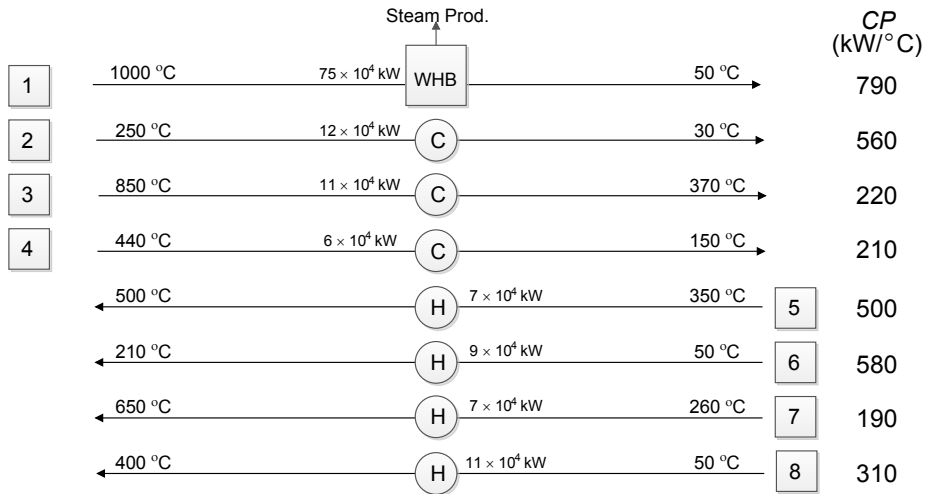


Figure 5.5: The initial heat and cooling demand for the Base Case Configuration.

The pinch temperature for this grid was determined by the use of the problem table method. [11] All the relevant data and calculations for this method are presented in Appendix D. The calculations showed that the available heat in the hot streams exceeded the energy needed to heat up the cold streams. This results was consistent for each temperature interval which gave a high pinch temperature: 1000 °C. The network design of heat exchangers was then designed below pinch where  $CP_h \geq CP_c$  needs to be satisfied. The suggested network design is presented in Figure 5.6. The red colour indicates that the stream is located in the hydrogen plant.

It would be beneficial for the synthesis gas production and hydrogen plant to be independent of each other. Any operation problems occurring in one of the facilities would cause production stop for both processes if they were interdependent. Thus, there was no heat exchange coupling across the different plants. Each of the heat exchangers' couplings as shown in Figure 5.6 will now be commented on.

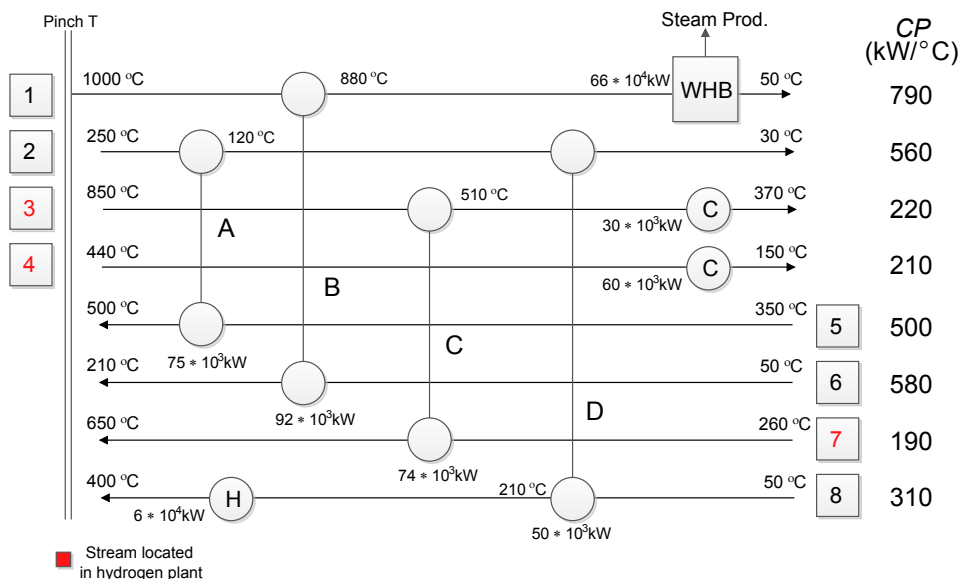


Figure 5.6: The proposed heat-exchanger network for Base Case Configuration. The grid was design below a pinch temperature of 1000°C.

### Heat Exchanger A

The pre-reformer outlet located in the synthesis gas production (stream 5) was coupled with the Fischer-Tropsch Outlet (stream 2), fulfilling the heat capacity flow requirement. This heat exchange eliminated the external energy requirement for stream 5.

### Heat Exchanger B

The Fischer-Tropsch inlet (stream 6) was coupled against the ATR outlet (stream 1). The ATR outlet had to be used for this coupling because it was the only stream with a sufficiently high  $CP_h$  value.

### Heat Exchanger C

The pre-reformer outlet (stream 7) needed an energy increase before it could enter the steam methane reformer. It was therefore coupled with the steam reformer outlet (stream 3).

### Heat Exchange D

The last cold stream that needed heating was the natural gas inlet entering the synthesis gas production (stream 8). This stream was heated up to 210°C by utilizing the remaining heat in the Fischer Tropsch outlet (stream 2). This heat improvement would reduce the needed size of the fire heater significantly, resulting in both lower investment and operational cost. This would also have a positive effect on the carbon efficiency in the system since the fire heater was fuelled by natural gas.

### Final Comments

The overall result from this network coupling shows a large improvement of the external energy input,  $Q$ . The main results related to energy efficiency are presented Table 5.9.

Table 5.9: Heat integration results for the Base Case Configuration.

	<b>Base Case</b>	<b>Base Case with Heat Integration</b>
Energy Efficiency [%]	7	9
Cooling demand [kW]	$29 \times 10^4$	$9 \times 10^4$
‡ of coolers	3	2
Total energy demand [kW]	$34 \times 10^4$	$6 \times 10^4$
External Input (Q) [kW]	$23 \times 10^4$	0
Fire Heater Demand [kW]	$11 \times 10^4$	$6 \times 10^4$
‡ of heaters	4	1
Fire Heater Demand [kW]	$11 \times 10^4$	$6 \times 10^4$
WHB Output [kW]	$75 \times 10^4$	$66 \times 10^4$

The energy efficiency increased from 7 to 9 % after this heat integration. All of these simulations only run once through the reactor, explaining the low initial value of 7 %. In an actual plant there would be included a recycle stream which



would give a larger increase in energy efficiency. A positive result from this heat integration is that the number of heaters was reduced from four to one: preheating of the natural gas entering the synthesis gas production. This single heater would in a actual plant be a natural gas driven fire heater. The energy demand of this heater was however reduced by 45 % because of the heat utilization occurring in heat exchanger D. The requirements for cooling equipment were also reduced, 3 to 2.

A even more detailed analysis of more cold and hot streams could have been conducted to improve this parameter further. The reason for including only eight streams is because this analysis is based on a limited product distribution. If more products and a recycle amounts had been implemented the energy analysis would also be different. The largest increase of carbon- and energy efficiency was achieved where both product and water was removed between each of the stages: Configuration 2. It would be interesting to investigate how this configuration could be improved, and an analysis of Configuration 2 is included in the next section.

### 5.3.2 Configuration 2

The natural gas ( $F_0$ ) distribution in this configuration is highly different from the Base Case. This changes the available energy in the various process streams. A new pinch analysis was conducted to find an optimal heat-exchange design. The pinch temperature calculations can be found in Appendix E. The available streams that would be utilized in this heat integration are the streams mentioned in section 4.4 together with the hot and cold streams listed below:

9. Fischer Tropsch Reactor 2 Outlet (Hot)
10. Fischer-Tropsch Reactor 3 Outlet (Hot)
11. Fischer Tropsch Reactor 2 Inlet (Cold)
12. Fischer Tropsch Reactor 3 Inlet (Cold)

These four streams (9-12) were included since Configuration 2 uses three PFRs in series with water and product separation between each of the reactors, as shown in Figure 4.2. The pinch temperature was found to be 1000°C and the heat exchanger network was designed below this pinch. This required that  $CP_h \geq CP_c$  was satisfied for all of the couplings, and the suggested network design for Configuration 2 is presented in Figure 5.7.

The synthesis gas and hydrogen streams were also here coupled separately to ensure independent processes. Below, all the heat exchangers' couplings related

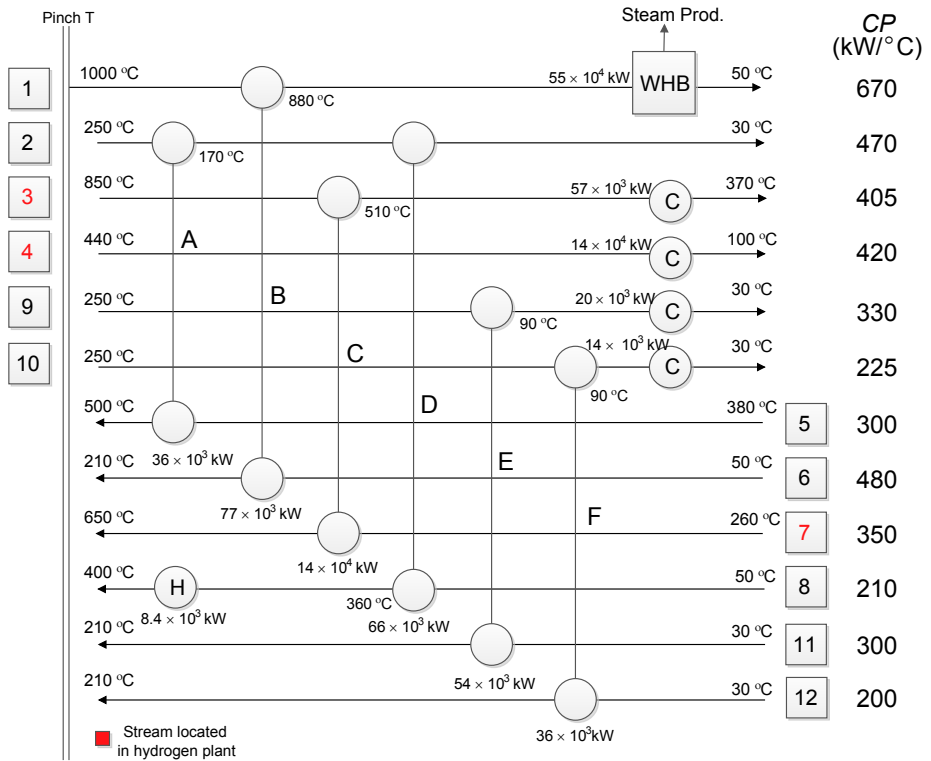


Figure 5.7: The proposed heat-exchanger network for Configuration 2. The grid was designed below a pinch temperature of 1000°C.

to Figure 5.7 will be outlined.

### Heat Exchanger A and B

The pre-reformer outlet located in the synthesis gas production (stream 5) was coupled with the F-T reactor outlet (stream 2) while the the F-T reactor inlet (stream 6) was coupled with the ATR outlet (stream 1). Because this fulfilling the heat capacity flow requirement.

### Heat Exchanger C

The ATR outlet was used for this coupling since this stream alone had a sufficiently high  $CP_h$  value of 670 [kW°C<sup>-1</sup>]. The hydrogen outlet stream which was located in the hydrogen plant (stream 7) was coupled with the steam reformer outlet (stream 3).

### Heat Exchanger D

The remaining energy present in the F-T reactor outlet 1 (stream 2) was used to heat up the natural gas entering the synthesis gas production (stream 8). This stream was heated up to 360 °C and would reduce the needed capacity of the fire heater significantly, resulting in both lower investment and operational cost. This effect would also improve the carbon efficiency of the system since the fire heater used natural gas as fuel.

### Heat Exchanger E and F

The F-T reactor 2 outlet could be used to heat up the F-T reactor inlet since  $CP_h \geq CP_c$  (330 against 300 kW°C<sup>-1</sup>). The same implementation was feasible for F-T reactor 3 where stream 10 was heat exchanged with stream 12.

### Final Comments

One interesting result from this network design is the large decrease in fire heater demand for the synthesis gas entering the synthesis gas production (stream 8). The CP value for this stream has decreased from 310 to 210 [kW°C<sup>-1</sup>] compared to the the Base Case, see Figure 5.6 and 5.7. The reason for this reduction is the difference in distribution of natural gas entering the system ( $F_0$ ). In Configuration 2 there is a larger amount of  $F_0$  being processed in the hydrogen plant, reducing the molar flow in stream 8. This results in a lower CP value.

It is important to mention a key assumption regarding this effect: The energy of the tail gas produced in the steam methane reformer (hydrogen plant) can be exploited to heat the natural gas that enters the hydrogen plant. This energy utilization in the hydrogen plant almost eliminates the need for a fire heat exchanger in Configuration 2.

### 5.3.3 Configuration Comparison

The heat integration improvements for the Base Case and Configuration 2 are presented in Table 5.10.

Table 5.10: Heat integration results: Base Case Configuration and Configuration 2.

	<b>Base Case</b>	<b>Base Case Heat Integr.</b>	<b>Conf. 2</b>	<b>Conf. 2 Heat Itegr.</b>
Energy Efficiency	7	9	13	19
Cooling demand [kW]	$29 \times 10^4$	$9 \times 10^4$	$90 \times 10^4$	$23 \times 10^4$
# of coolers	3	2	5	4
TOT energy demand [kW]	$34 \times 10^4$	$6 \times 10^4$	$49 \times 10^4$	$8.4 \times 10^3$
External Input (Q)	$23 \times 10^4$	0	$42 \times 10^4$	0
Fire Heater Demand	$11 \times 10^4$	$6 \times 10^4$	$7 \times 10^4$	$8.4 \times 10^3$
# of heaters	4	1	6	1
WHB Output [kW]	$75 \times 10^4$	$66 \times 10^4$	$64 \times 10^4$	$55 \times 10^4$

Configuration 2 has a higher initial energy efficiency than the Base Case: 13 against 7 %. This is because the production amounts were 17.9 % higher in this configuration. The final heat integration result show that the heat utilization had a greater effect in Configuration 2 then than in the Base Case Configuration. This is explained by the difference in total energy demand of the two different configurations. The reduction in external energy input (Q) in Configuration 2 is almost twice the reduction amount of the Base Case.

The downsides of Configuration 2 is the increase in cooling demand. It is also necessary to buy two additionally coolers which increases the investment cost. Configuration also gives a 17 % decrease in waste heat boiler (WHB) output which reduced the ability to produce electrical power generation. The increase in investment cost and reduction in steam generation is regarded as less important since the overall objective is to increase mass product, which Configuration 2 does.

## 5.4 Future work

The kinetic model by Todic et al.[2] describes the actual production distribution. The implementation of this model proved to be more difficult than expected since

each of the reactions had to be implemented separately. The product distribution was therefore limited to 29 products for the simulation to converge. This simplification affects the results considerably since the consumption of CO would be higher if more products were included. It would thus be desirable to find a different way of implementing the suggested kinetic with even products to give a better representation of CO consumption and product distribution occurring in an actual gas-to-liquid plant.

To improve the overall efficiency of the process it would be interesting to examine the effect on carbon efficiency and products amount if unconverted reactants were recycled. One streams could be processed in the synthesis gas production while the other unconverted synthesis gas would be processed in the F-T synthesis. The distribution of these two streams should be approached as an optimization problem.

It would also be desirable to find an optimal capacity for a given GTL plant. This could be achieved by conducting a more detailed economical study where both the capital and operational costs would be compared with production amounts.



# Chapter 6

## Conclusion

This master's thesis has considered three different GLT-configurations. The simulations that were conducted revealed that Configuration 2 was the most optimal design for production of longer hydrocarbon chains. The justifications for this choice were:

- Highest production of products was achieved, 30 000 barrels/day.
- The highest carbon-and energy efficiency was accomplished. These were respectively 31 % and 13 %.
- Exploiting a CO<sub>2</sub> rich tail gas from the hydrogen plant gave an increase in the overall efficiency since more carbon could be converted to the desired products. Pollution emission regarding this stream was also eliminated because this stream was utilized for synthesis gas production.
- Processing a synthesis gas with lower H<sub>2</sub>/CO ratio reduced the methane production by 20 % compared with the Base Case Configuration.
- The required oxygen demand in the synthesis gas production was reduced by 23% when comparing it with the Base Case Configuration.
- Heat integration in the form of a optimal heat exchange network made the largest increase in energy efficiency when compared with the Base Case Configuration. This was from 13 to 19 %. As a result the heat requirement for preheating the natural gas entering the synthesis gas plant was almost neglected.





# Bibliography

- [1] RAFIEE, A. and M. HILLESTAD: Synthesis Gas Production Configuration for Gas-to-Liquid Applications. *Chemical Engineering Technology*, 35(5):870–876, 2012.
- [2] TODIC, B., W. MA, G. JACOBS, B.H. DAVIS and D. B. BUKUR: CO-insertion mechanism based kinetic model of the Fischer-Tropsch synthesis reaction over Re-promoted CO catalyst. *Catalysis Today* 2013.
- [3] KLERK, A. D.: Fischer-Tropsch Refining. *WILEY-VCH Verlag GmbH & Co. KgaA, Weinheim*, 1. edition, 2011.
- [4] BOYCE, C.A., A.M. CREWS and R. RITTER: Time for a new hydrogen plant? *Hydrocarbon Engineering*, pages 67–70, 2004.
- [5] CHORKENDORFF, I. and J.W. NIEMANTSVERDRIET: Concepts of Modern Catalysis and Kinetics. *WILEY-VCH Verlag GmbH & Co. KgaA, Weinheim*, 2 edition, 2007.
- [6] DRY, M.E.: The Fischer–Tropsch process: 1950–2000. *Catalysis Today*, 71(3-4):227–241, January 2002.
- [7] BAKKERUD, P.K.: Update on synthesis gas production for GTL. *Catalysis Today*, 106:30–33, 2005.
- [8] PENDYALA, V.R.R., G. JACOBS, W. MA, J. L. S. KLETTLINGER, C.H. YEN and B.H. DAVIS: Fischer–Tropsch synthesis: Effect of catalyst particle (sieve) size range on activity, selectivity, and aging of a Pt promoted Co/Al<sub>2</sub>O<sub>3</sub> catalyst. *Chemical Engineering Journal*, 249:279–284, August 2014.
- [9] MOULIJN, J.A., M. MAKKEE and A. VAN DIEPEN: Chemical Process Technology. *John Wiley & Sons Ltd, Chichester*, 1 edition, 2001.

- [10] STORSÆTER, S., D. CHEN and A. HOLMEN: Microkinetic modelling of the formation of C<sub>1</sub> and C<sub>2</sub> products in the Fischer–Tropsch synthesis over cobalt catalysts. *Surface Science*, 600(10):2051–2063, May 2006.
- [11] SINNOTT, R. and G. TOWLER: Chemical Engineering Design. *Elsevier Ltd., Oxford*, 5 edition, 2009.
- [12] PETRUCCI, R.H., W.S. HARDWOOD, F. GEOFFREY HERRING and J.D. MADURA: General Chemistry: Principles & Modern Applications. *Pearson Education Inc.*, New Jersey, Ninth edition, 2007.
- [13] HILLESTAD, M.: *personal communication*.

# Appendix A

## MATLAB Kinetic Script

There are included different MATLAB scripts in this Appendix to calculate the production rates given by the published kinetic model by Todić et al. [2]. The reason for this implementation was to confirm similar rates as the article presents.

The overall structure of this MATLAB calculation is given by a main script which calls four different functions:

- function  $k = \text{rateconstants}(T)$ : Calculates the equilibrium and reaction rate constants for a given temperature
- function  $g = \text{cost}(S, P_{\text{CO}}, P_{\text{H}_2}, P_{\text{H}_2\text{O}}, T, n)$ : This is the whole expression for vacant active site on catalyst and is referred to as the cost function.
- function  $al = \text{alpha}(T, P_{\text{CO}}, P_{\text{H}_2}, P_{\text{H}_2\text{O}}, S, n)$ : Calculates all the different chain growth probabilities for carbon number  $n$ .
- function  $\text{root} = \text{regulafalsi}(f, a, b, \text{epsilon})$ : The mathematical method for solving the implicit cost function.

The inputs for the main scripts are:

- Partial pressure of  $\text{H}_2$  [MPa]
- Partial pressure of  $\text{CO}$  [MPa]
- Partial pressure of  $\text{H}_2\text{O}$  [MPa]
- Temperature [K]
- Number of products  $n$

All of these are included in the first lines of the main scripts before the cost function is called. This function contains the whole expression that describes the vacant sites at the catalyst,  $S$ . Both the constants and the alpha function is called in this function which calculates the needed chain growth probabilities, equilibrium and reaction rate constants. This expression is an implicit function meaning that  $S=f(S)$ . It is therefore necessary to have established the function  $f$  before the iteration of  $S$  could start. This is achieved by the use of a method called regula falsi, see regula falsi function below. It guesses "false" values for the different variables and adjusts the different values until the tolerance limit is reached. This limit is called epsilon in the regulafalsi function and have a value of 0.001. When the appropriate approximation of  $S$  is found the different production rates can be calculated.

```

1  %Main Script
2
3  %Process Conditions. Pressure [MPa], Temperature [K]
4  P_H2=0.99;
5  P_CO=0.49;
6  P_H2O=0.0;
7  T=478.15;
8  n=15;
9
10 % Function f
11 f = @(S) cost(S,P_CO,P_H2,P_H2O,T,n)
12
13 % Solving for S
14 root = regulafalsi(f,0,1)
15 S=root
16
17 %Reaction and Equilibrium constants
18 k = rateconstants(T);
19
20 %Calculation of Alpha Values
21 al = alpha(T,P_CO,P_H2,P_H2O,S,n);
22
23
24 %Rate expression for Methane production
25 R_Metan=k.k7M*(k.K2^0.5)*(P_H2^0.5)*al(1)*(S^2);
26
27
28 %Rate expression for alkanes production
29 B1=k.k7*(k.K2^0.5)*(P_H2^0.5)*al(1)*S^2;
30
31 for i=2:n;
32     Ralkaner(i)=B1*al(i);
33     B1=Ralkaner(i);
34 end
35

```

```

36 Ralkaner=Ralkaner(2:n);
37
38 %Rate expression for Ethane production
39 R_C2H2=k.k8E*exp(-0.27*2)*al(1)*al(2)*S;
40
41 %Rate expression for Alkenes production
42 B2=k.k8*al(1)*al(2)*S;
43
44 for i=3:n;
45     Ralkaner(i)=B2*al(i);
46     B2=Ralkaner(i);
47 end
48
49 for i=3:n;
50     Ralkaner(i)=Ralkaner(i)*exp(-0.27*i);
51 end
52
53 %Result Rates
54 ResultsAlkaner=[R_Metan Ralkaner]';
55 ResultsAlkener=[0 R_C2H2 Ralkaner(3:15)]';

```

```

1 function g = cost(S, P_CO,P_H2,P_H2O,T,n )
2
3
4 k=rateconstants(T);
5 al=alpha(T,P_CO,P_H2,P_H2O,S,n);
6
7 mem1=1+k.K1*P_CO+sqrt(k.K2*P_H2);
8
9 mem2=(1/((k.K2^2)*k.K4*k.K5*k.K6)*(P_H2O/(P_H2^2)))+sqrt(k.K2*P_H2)
10
11 M=1; Q=0;
12 for i=1:n;
13     M=M*al(i);
14     Q=Q+M;
15 end
16
17 f = 1.0/(mem1 + Q*mem2);
18 g=S-f;
19 end

```

```

1 function k = rateconstants(T)
2
3 % Temperature are expressed in Kelvin
4
5 k.K1 = 6.59e-5*exp(48.9e3/(8.314*T));
6 k.K2 = 1.64e-4*exp(9.4e3/(8.314*T));
7 k.k3 = 4.14e8 *exp(-92.8e3/(8.314*T));

```

```

8 k.K4 = 3.59e5 *exp(-16.2e3/(8.314*T));
9 k.K5 = 9.81e-2*exp(-11.9e3/(8.314*T));
10 k.K6 = 1.59e6 *exp(-14.5e3/(8.314*T));
11 k.k7 = 4.53e7 *exp(-75.5e3/(8.314*T));
12 k.k8 = 4.11e8 *exp(-100.4e3/(8.314*T));
13 k.k7M= 7.35e7 *exp(-65.4e3/(8.314*T));
14 k.k8E= 4.60e7 *exp(-103.2e3/(8.314*T));
15
16 end

```

```

1 function al = alpha(T,P_CO,P_H2,P_H2O,S,n)
2 al=zeros(n,1);
3 k=rateconstants(T);
4 %Alpha 1
5 al(1) = k.k3*k.K1*P_CO / (k.k3*k.K1*P_CO + k.k7M*sqrt(k.K2*P_H2));
6 %Alpha 2
7 al(2) = k.k3*k.K1*P_CO*S / ( k.k3*k.K1*P_CO*S + ...
8     k.k7*sqrt(k.K2*P_H2)*S + k.k8E*exp(-0.27*2 ) );
9 %Alpha 3+
10 for i=3:n
11     al(i)=k.k3*k.K1*P_CO*S/(k.k3*k.K1*P_CO*S+k.k7*sqrt(k.K2*P_H2)
12     *S+k.k8*exp(-0.27*i));
13 end
14 end

```

```

1 function root = regulafalsi(f,a,b,epsilon)
2
3     Iter = 0;
4     epsilon = 0.001;
5     g = 1;
6     while(g > epsilon)
7         Iter = Iter + 1;
8         x = a - ((f(a)*(b-a))/(f(b) - f(a)));
9         if(f(x)*f(a) > 0)
10            b = x;
11            g = f(b);
12            root = b;
13        else
14            a = x;
15            g = f(a);
16            root = a;
17        end
18    end
19 end

```

## Appendix B

# DLL Extension code for pentene

This Appendix contains the complete extension code for pentene. This code is written with the Visual Basic 6 software, and consists of a main module that calls a sub routine (Option Explicit).

```
1  'Propene Reaction Extension
2  '-----
3
4  'Require that all variables used be declared.  This is good ...
   'practice as it helps
5  Option Explicit
6
7  'Declare global HYSYS objects
8  Dim hyContainer As Object
9  Dim hyBulkDens As Object
10
11
12
13  'Initialize
14  Public Function Initialize(ByVal Container As Object, ByVal ...
   'IsRecalling As Boolean) As Long
15
16  'Enable error trapping'
17  On Error GoTo ErrorTrap
18
19  'Declare local HYSYS objects'
20  Dim hyReactant As Reactant
21
```

```

22 'Reference the current HYSYS version'
23     Initialize = extnCurrentVersion
24
25 'Reference the Container object which called the extension'
26     Set hyContainer = Container
27
28 'Set an object reference to the BulkDens variable in the EDF'
29     Set hyBulkDens = hyContainer.FindVariable("BulkDens").Variable
30
31 'IsRecalling is only False when the extension is first added to ...
    the simulation'
32     If IsRecalling = False Then
33         'Default values for BulkDens (2700 kg catalyst/m3 reactor ...
            volume)
34         hyBulkDens.Value = 550
35
36 'Reaction properties'
37     hyContainer.Phase = ptVapourPhase 'Vapour phase reaction
38     hyContainer.ReactionBasis = rbPartialPressBasis 'Partial ...
            pressure reaction
39
40 'Remove all reactants'
41     hyContainer.Reactants.RemoveAll
42
43 'Add desired reactants and set their stoichiometric value'
44     Set hyReactant = hyContainer.Reactants.Add("CO")
45     hyReactant.StoichiometricCoefficientValue = -3
46 'Set CO as the base reactant used in the rate equation'
47     hyContainer.BaseReactant = hyReactant
48     Set hyReactant = hyContainer.Reactants.Add("Hydrogen")
49     hyReactant.StoichiometricCoefficientValue = -6
50     Set hyReactant = hyContainer.Reactants.Add("Propene")
51     hyReactant.StoichiometricCoefficientValue = 1
52     Set hyReactant = hyContainer.Reactants.Add("H2O")
53     hyReactant.StoichiometricCoefficientValue = 3
54
55     'Set BasisConversion units'
56     hyContainer.BasisConversion = "MPa"
57
58 'Set the property state as calculated so that they cannot be ...
    modified'
59     With hyContainer
60         .SetReactionPropertyState rpReactants, vsCalculated
61         .SetReactionPropertyState ...
            rpStoichiometricCoefficients, vsCalculated
62         .SetReactionPropertyState rpMinTemperature, vsCalculated
63         .SetReactionPropertyState rpMaxTemperature, vsCalculated
64         .SetReactionPropertyState rpReactionBasis, vsCalculated
65         .SetReactionPropertyState rpReactionPhase, vsCalculated
66         .SetReactionPropertyState rpBaseReactant, vsCalculated
67         .SetReactionPropertyState rpBasisConversion, vsCalculated
68         .SetReactionPropertyState rpRateConversion, vsCalculated

```



```

69     End With
70
71     End If
72
73     'Line to which the On Error statment branches if an error occurs'
74     ErrorTrap:
75
76     End Function
77
78
79     'Reactionrate is called whenever the extension is executed'
80
81     Public Function ReactionRate(ByVal Fluid As Object, ByVal ...
82         RxnTemperatureInC As Double, ByVal RxnVolumeInKmolPerM3 As ...
83         Double, rate As Double) As Boolean
84
85         'Enable error trapping'
86         On Error GoTo ErrorTrap
87
88         'Declare local variables'
89         Dim TotalPressure As Double
90         Dim RxnTemperatureinK As Double
91         Dim COIndex As Integer
92         Dim HydrogenIndex As Integer
93         Dim PropeneIndex As Integer
94         Dim H2OIndex As Integer
95         Dim ComponentFrac As Variant
96         Dim COPP As Double
97         Dim HydrogenPP As Double
98         Dim PropenePP As Double
99         Dim H2OPP As Double
100        Dim S As Double
101        Dim alpha1 As Double
102        Dim alpha2 As Double
103        Dim alpha3 As Double
104
105        'Number of carbons generated'
106        Dim n As Integer
107        n = 15
108
109        'Check hyBulkDens, if <=0 then set to default value of 2700 kg ...
110        catalyst/m3 reactor volume'
111
112        If hyBulkDens.Value <= 0 Then hyBulkDens.Value = 550
113
114        'Get the overall pressure in PSIA at which the reaction is occurring'
115        TotalPressure = Fluid.Pressure.GetValue("MPa")
116
117        'Get the reaction temperature in K'
118        RxnTemperatureinK = RxnTemperatureInC + 273.15
119
120        'Get component index numbers'

```

```

118     COIndex = Fluid.Components.Index("CO")
119     HydrogenIndex = Fluid.Components.Index("Hydrogen")
120     PropeneIndex = Fluid.Components.Index("Propene")
121     H2OIndex = Fluid.Components.Index("H2O")
122
123     'Set ComponentFrac equal to the component molar fractions of the ...
        fluid'
124     ComponentFrac = Fluid.MolarFractionsValue
125
126     'Get partial pressure of components in PSIA by multiplying ...
        component mole fraction by total pressure'
127     COPP = ComponentFrac(COIndex) * TotalPressure
128     HydrogenPP = ComponentFrac(HydrogenIndex) * TotalPressure
129     PropenePP = ComponentFrac(PropeneIndex) * TotalPressure
130     H2OPP = ComponentFrac(H2OIndex) * TotalPressure
131
132
133     'Constants, K1—K8E and Alpha'
134     Dim K1 As Double
135     Dim K2 As Double
136     Dim K3 As Double
137     Dim K4 As Double
138     Dim K5 As Double
139     Dim K6 As Double
140     Dim K7 As Double
141     Dim K8 As Double
142     Dim K7M As Double
143     Dim K8E As Double
144
145     K1 = 0.0000659 * Exp(48.9 / (0.008314 * RxnTemperatureinK))
146     K2 = 0.000164 * Exp(9.4 / (0.008314 * RxnTemperatureinK))
147     K3 = 414000000 * Exp(-92.8 / (0.008314 * RxnTemperatureinK))
148     K4 = 359000 * Exp(-16.2 / (0.008314 * RxnTemperatureinK))
149     K5 = 0.0981 * Exp(-11.9 / (0.008314 * RxnTemperatureinK))
150     K6 = 1590000 * Exp(-14.4 / (0.008314 * RxnTemperatureinK))
151     K7 = 45300000 * Exp(-75.5 / (0.008314 * RxnTemperatureinK))
152     K8 = 411000000 * Exp(-100.4 / (0.008314 * RxnTemperatureinK))
153     K7M = 73500000 * Exp(-65.4 / (0.008314 * RxnTemperatureinK))
154     K8E = 46000000 * Exp(-103.2 / (0.008314 * RxnTemperatureinK))
155
156
157     'Implemented Kinetic Model Todici et al.'
158
159     Dim regf As Regulafalsi
160     Set regf = New Regulafalsi
161
162     regf.RxnTemperatureinK = RxnTemperatureinK
163     regf.COPP = COPP
164     regf.HydrogenPP = HydrogenPP
165     regf.H2OPP = H2OPP
166     regf.n = 15
167     regf.A = 0

```

```

168     regf.B = 1
169     regf.Epsilon = 0.001
170
171     S = regf.CalculatesS      'Calls function from Sub Module and ...
                             Calculates S'
172
173
174     'Alpha Values'
175     alpha1 = K3 * K1 * COPP / (K3 * K1 * COPP + K7M * Sqr(K2 * ...
                             HydrogenPP))
176     alpha2 = K3 * K1 * COPP * S / (K3 * K1 * COPP * S + K7 * ...
                             Sqr(K2 * HydrogenPP) * S + K8E * Exp(-0.27 * 2))
177     alpha3 = K3 * K1 * COPP * S / (K3 * K1 * COPP * S + K7 * ...
                             Sqr(K2 * HydrogenPP) * S + K8 * Exp(-0.27 * 3))
178
179     'Propene rate'
180     rate = K8 * Exp(-0.27 * 3) * S * alpha1 * alpha2 * alpha3
181
182     'Conversion to correct units kgmole/m3-s and CO consumption '
183     rate = rate * hyBulkDens.Value * 3 / 3600
184
185     'Tell HYSYS that the calculation worked as expected'
186     ReactionRate = True
187
188     'Line to which the On Error statement branches if an error occurs'
189     ErrorTrap:
190
191     'Tell HYSYS that the calculation did not work as expected'
192
193     ReactionRate = False
194
195     End Function

```

```

1  Option Explicit
2
3  'Variables'
4  Dim K1 As Double
5  Dim K2 As Double
6  Dim K3 As Double
7  Dim K4 As Double
8  Dim K5 As Double
9  Dim K6 As Double
10 Dim K7 As Double
11 Dim K8 As Double
12 Dim K7M As Double
13 Dim K8E As Double
14 Dim m_A As Double
15 Dim m_B As Double
16 Dim m_Epsilon As Double
17

```

```
18 'Variables for cost calculation'
19 Dim m_RxnTemperatureinK As Double
20 Dim m_COPP As Double
21 Dim m_HydrogenPP As Double
22 Dim m_H2OPP As Double
23 Dim m_n As Integer
24
25
26 'Rate and Equilibrium Constants'
27 Public Property Let RxnTemperatureinK(ByVal NewVal As Double)
28     m_RxnTemperatureinK = NewVal
29     CalculateK (NewVal)
30 End Property
31 Public Property Let COPP(ByVal NewVal As Double)
32     m_COPP = NewVal
33 End Property
34 Public Property Let HydrogenPP(ByVal NewVal As Double)
35     m_HydrogenPP = NewVal
36 End Property
37 Public Property Let H2OPP(ByVal NewVal As Double)
38     m_H2OPP = NewVal
39 End Property
40 Public Property Let n(ByVal NewVal As Integer)
41     m_n = NewVal
42 End Property
43 Public Property Let A(ByVal NewVal As Double)
44     m_A = NewVal
45 End Property
46 Public Property Let B(ByVal NewVal As Double)
47     m_B = NewVal
48 End Property
49 Public Property Let Epsilon(ByVal NewVal As Double)
50     m_Epsilon = NewVal
51 End Property
52 Public Property Get COPP_1() As Double
53     COPP_1 = m_COPP
54 End Property
55
56 Public Sub CalculateK(ByVal RxnTemperatureinK As Double)
57     K1 = 0.0000659 * Exp(48.9 / (0.008314 * m_RxnTemperatureinK))
58     K2 = 0.000164 * Exp(9.4 / (0.008314 * m_RxnTemperatureinK))
59     K3 = 414000000 * Exp(-92.8 / (0.008314 * m_RxnTemperatureinK))
60     K4 = 359000 * Exp(-16.2 / (0.008314 * m_RxnTemperatureinK))
61     K5 = 0.0981 * Exp(-11.9 / (0.008314 * m_RxnTemperatureinK))
62     K6 = 1590000 * Exp(-14.4 / (0.008314 * m_RxnTemperatureinK))
63     K7 = 45300000 * Exp(-75.5 / (0.008314 * m_RxnTemperatureinK))
64     K8 = 411000000 * Exp(-100.4 / (0.008314 * m_RxnTemperatureinK))
65     K7M = 73500000 * Exp(-65.4 / (0.008314 * m_RxnTemperatureinK))
66     K8E = 46000000 * Exp(-103.2 / (0.008314 * m_RxnTemperatureinK))
67 End Sub
68
69 'S Function'
```

```

70 Public Function F(ByVal S As Double) As Double
71
72 Dim M, Q, Mem1, Mem2, g As Double
73 Dim i As Integer
74 Dim alpha(1 To 15) As Double
75 Call GetAlpha(alpha, S)
76
77 Mem1 = 1 + K1 * m.COPP + Sqr(K2 * m.HydrogenPP)
78
79 Mem2 = (1 / ((K2 ^ 2) * K4 * K5 * K6) * (m.H2OPP / (m.HydrogenPP ...
      ^ 2))) + Sqr(K2 * m.HydrogenPP)
80
81 M = 1
82 Q = 0
83 i = 1
84
85 Do While i ≤ 15
86     M = M * alpha(i)
87     Q = M + Q
88     i = i + 1
89 Loop
90
91 g = 1# / (Mem1 + (Q * Mem2))
92
93 F = S - g
94
95 End Function
96
97 'Regula Falsi Function'
98
99 Public Function CalculatesS() As Double
100     Dim Iter As Integer
101     Dim g, x, root As Double
102
103     If K1 = 0 Then
104         MsgBox ("No constants set for temp")
105         Exit Function
106     End If
107
108     Iter = 0
109     g = 1
110
111     Do While g > m.Epsilon
112         Iter = Iter + 1
113         If F(m_A) = F(m_B) Then
114             'Function has the same value on a and b on iteration'
115         End If
116         x = m_A - ((F(m_A) * (m_B - m_A)) / (F(m_B) - F(m_A)))
117         If F(x) * F(m_A) > 0 Then
118             m_B = x
119             g = F(m_B)
120             root = m_B

```

```
121         Else
122             m_A = x
123             g = F(m_A)
124             root = m_A
125         End If
126     Loop
127     CalculateS = root
128
129 End Function
130
131 'Alpha Function'
132
133 Public Sub GetAlpha(alpha() As Double, ByRef S As Double)
134
135     Dim i As Integer
136
137     alpha(1) = K3 * K1 * m_COPP / (K3 * K1 * m_COPP + K7M * Sqr(K2 * ...
        m_HydrogenPP))
138
139     alpha(2) = K3 * K1 * m_COPP * S / (K3 * K1 * m_COPP * S + K7 * ...
        Sqr(K2 * m_HydrogenPP) * S + K8E * Exp(-0.27 * 2))
140
141     i = 3
142     Do While i ≤ 15
143         alpha(i) = K3 * K1 * m_COPP * S / (K3 * K1 * m_COPP * S + K7 * ...
            * Sqr(K2 * m_HydrogenPP) * S + K8 * Exp(-0.27 * i))
144         i = i + 1
145     Loop
146
147 End Sub
```

# Appendix C

## MATLAB to HYSYS Implementation Data

The MATLAB and UNISIM rate comparison tables are presented in Table C.1 and C.2. The test shows that the deviations between the programs are small, which confirms correct implementation of the given model.

Table C.1: Alkanes reaction rates comparison between MATLAB and HYSYS

Component	Reaction Rate	Reaction Rate
	MATLAB [mol g <sub>cat</sub> <sup>-1</sup> h <sup>-1</sup> ]	HYSYS [mol g <sub>cat</sub> <sup>-1</sup> h <sup>-1</sup> ]
Methane	1.56 · 10 <sup>-3</sup>	1.74 · 10 <sup>-3</sup>
Ethane	7.18 · 10 <sup>-5</sup>	7.10 · 10 <sup>-5</sup>
Propane	6.37 · 10 <sup>-5</sup>	6.32 · 10 <sup>-5</sup>
Butane	5.75 · 10 <sup>-5</sup>	5.72 · 10 <sup>-5</sup>
Pentane	5.25 · 10 <sup>-5</sup>	5.24 · 10 <sup>-5</sup>
Hexane	4.85 · 10 <sup>-5</sup>	4.85 · 10 <sup>-5</sup>
Heptane	4.51 · 10 <sup>-5</sup>	4.52 · 10 <sup>-5</sup>
Octane	4.21 · 10 <sup>-5</sup>	4.23 · 10 <sup>-5</sup>
Nonane	3.96 · 10 <sup>-5</sup>	3.98 · 10 <sup>-5</sup>
Decane	3.73 · 10 <sup>-5</sup>	3.75 · 10 <sup>-5</sup>
C <sub>11</sub> H <sub>24</sub>	3.52 · 10 <sup>-5</sup>	3.55 · 10 <sup>-5</sup>
C <sub>12</sub> H <sub>26</sub>	3.33 · 10 <sup>-5</sup>	3.36 · 10 <sup>-5</sup>
C <sub>13</sub> H <sub>28</sub>	3.16 · 10 <sup>-5</sup>	3.19 · 10 <sup>-5</sup>
C <sub>14</sub> H <sub>30</sub>	3.00 · 10 <sup>-5</sup>	3.03 · 10 <sup>-5</sup>
C <sub>15</sub> H <sub>32</sub>	2.85 · 10 <sup>-5</sup>	2.88 · 10 <sup>-5</sup>

Table C.2: Alkenes reaction rates comparison between MATLAB and HYSYS

Component	Reaction Rate	Reaction Rate
	MATLAB [mol g <sub>cat</sub> <sup>-1</sup> h <sup>-1</sup> ]	HYSYS [mol g <sub>cat</sub> <sup>-1</sup> h <sup>-1</sup> ]
Ethylene	8.01 · 10 <sup>-6</sup>	7.94 · 10 <sup>-6</sup>
Propen	9.81 · 10 <sup>-5</sup>	9.76 · 10 <sup>-5</sup>
Butene	6.76 · 10 <sup>-5</sup>	6.72 · 10 <sup>-5</sup>
Penten	4.71 · 10 <sup>-5</sup>	4.69 · 10 <sup>-5</sup>
Hexen	3.32 · 10 <sup>-5</sup>	3.31 · 10 <sup>-5</sup>
Hepten	2.35 · 10 <sup>-5</sup>	2.35 · 10 <sup>-5</sup>
Octen	1.68 · 10 <sup>-5</sup>	1.68 · 10 <sup>-5</sup>
Nonen	1.21 · 10 <sup>-5</sup>	1.20 · 10 <sup>-5</sup>
Decen	8.68 · 10 <sup>-6</sup>	8.65 · 10 <sup>-6</sup>
C <sub>11</sub> H <sub>22</sub>	6.26 · 10 <sup>-6</sup>	6.24 · 10 <sup>-6</sup>
C <sub>12</sub> H <sub>24</sub>	4.52 · 10 <sup>-6</sup>	4.52 · 10 <sup>-6</sup>
C <sub>13</sub> H <sub>26</sub>	3.27 · 10 <sup>-6</sup>	3.27 · 10 <sup>-6</sup>
C <sub>14</sub> H <sub>28</sub>	2.37 · 10 <sup>-6</sup>	2.37 · 10 <sup>-6</sup>
C <sub>15</sub> H <sub>30</sub>	1.72 · 10 <sup>-6</sup>	1.72 · 10 <sup>-6</sup>



## Appendix D

# Pinch analysis: Base Case Configuration

The pinch temperature for this grid was determined by the use of the: "Problem Table Method".[11] This specific method is presented in more detail in section in section 4.4. The average heat capacity flow ( $CP$ ) for each of the streams was collected from the HYSYS simulation and are all presented in Table D.1

Table D.1: Average heat-capacity flow rate values : Base Case Configuration.

<b>Hot Stream</b>	$CP$ [kW/°C]	<b>Cold Streams</b>	$CP$ [kW/°C]
1	790	5	500
2	560	6	580
3	220	7	190
4	210	8	310

All streams were then arranged after the highest interval temperature of 995°C to the lowest of 25 °C. An energy balance for each of the temperature intervals was performed, see Table D.2.

The sum of heat capacities of all the cold streams in each of the temperature intervals was then calculated, the same was done for the hot streams. The difference between these two values would give an indication where the pinch is located. These calculations are presented in Table D.3.

There is excess heat in almost all of the different intervals. Only in the interval

Table D.2: Ranked order of the different temperature intervals for the Base Case Configuration. The energy balances for each of the intervals are also included.

<b>Rank</b>	Interval $\Delta T_n$ [ $^{\circ}\text{C}$ ]	Streams in interval
995 $^{\circ}\text{C}$		
845	150	-1
655	190	-(1+3)
505	150	7-(1+3)
435	70	(5+7)-(1+3)
405	30	(5+7)-(1+3+4)
365	40	(5+7+8)-(1+3+4)
355	10	(5+7+8)-(1+4)
265	90	(7+8)-(1+4)
245	20	8-(1+4)
215	30	8-(1+2+4)
145	70	(6+8)-(1+2+4)
55	90	(6+8)-(1+2)
45	10	-(1+2)
25	20	-2

Table D.3: Main pinch analysis table for the Base Case Configuration.

<b>Interval</b>	Interval Temp	$\Delta T_n$ [ $^{\circ}\text{C}$ ]	$\sum CP_c - \sum CP_h$ [kW/ $^{\circ}\text{C}$ ]	$\Delta H$ [kW]
995 $^{\circ}\text{C}$				
1	845	150	-790	$\approx -1.2 \times 10^5$
2	655	190	-1010	$\approx -1.9 \times 10^5$
3	505	150	-820	$\approx -1.2 \times 10^5$
4	435	70	-320	$\approx -2.2 \times 10^4$
5	405	30	-530	$\approx -1.6 \times 10^4$
6	365	40	-220	$\approx -8.8 \times 10^3$
7	355	10	0	0
8	265	90	-500	$\approx -4.5 \times 10^4$
9	245	20	-270	$\approx -5.4 \times 10^3$
10	215	30	-1250	$\approx -3.8 \times 10^4$
11	145	70	-670	$\approx -4.7 \times 10^4$
12	55	90	-460	$\approx -4.1 \times 10^4$
13	45	10	-1350	$\approx -1.35 \times 10^4$
14	25	20	-560	$\approx -1.1 \times 10^4$

355-365°C is the difference zero. This large availability indicates that the pinch temperature for this specific system was high. It was therefore decided that the network configuration would be designed below a pinch temperature of 1000°C.



# Appendix E

## Pinch analysis: Configuraration 2

The pinch temperature for this grid was determined by use of the "Problem Table Method".[11] This specific method is presented in more detail in section in section 4.4. The average heat capacity flow ( $CP$ ) for each of the streams was collected from the HYSYS simulation and are all presented in Table E.1.

Table E.1: Average heat-capacity flow rate values: Configuration 2.

<b>HOT Streams</b>	$CP$ [kW/°C]	<b>COLD Streams</b>	$CP$ [kW/°C]
1	670	5	300
2	470	6	480
3	405	7	350
4	420	8	210
9	330	11	300
10	225	12	200

All the streams were then arranged after the highest interval temperature 995°C to the lowest, 25 °C. An energy balance for each of the temperature intervals was performed, see Table E.2.

The sum of heat capacities of all the cold streams in each of the temperature intervals was then calculated, the same was done for the hot streams. The difference between these two values gave an indication of where the pinch is located.

Table E.2: Ranked order of the different temperature intervals for Configuration 2. The energy balances for each of the intervals are also included.

Rank	Interval $\Delta T_n(^{\circ}C)$	Streams in interval
995 $^{\circ}C$		
845	150	-1
655	190	-(1+3)
505	150	7-(1+3)
435	70	(5+7)-(1+3)
405	30	(5+7)-(1+3+4)
385	20	(5+7+8)-(1+3+4)
365	20	(7+8)-(1+3+4)
265	100	(7+8)-(1+4)
245	20	8-(1+4)
215	30	8-(1+2+4+9+10)
95	120	(6+8+11+12)-(1+2+4+9+10)
55	40	(6+8+11+12)-(1+2+9+10)
45	10	(11+12)-(1+2+9+10)
35	10	(11+12)-(2+9+10)
25	20	-(2+9+10)

These calculation are presented in Table E.3.

Table E.3: Main pinch analysis table for Configuration 2.

Interval	Interval Temp	$\Delta T_n$ [ $^{\circ}C$ ]	$\sum CP_c - \sum CP_h$ [kW/ $^{\circ}C$ ]	$\Delta H$ [kW]
995 $^{\circ}C$				
1	845	150	-670	$\approx -1 \times 10^5$
2	655	190	-1075	$\approx -2 \times 10^5$
3	505	150	-725	$\approx -1.1 \times 10^5$
4	435	70	-425	$\approx -3 \times 10^4$
5	405	30	-530	$\approx -1.6 \times 10^4$
6	385	20	-845	$\approx -1.7 \times 10^4$
7	365	20	-895	$\approx -1.8 \times 10^4$
8	265	100	-530	$\approx -5.3 \times 10^4$
9	245	20	-880	$\approx -1.8 \times 10^4$
10	215	30	-1950	$\approx -5.7 \times 10^4$
11	95	120	-1250	$\approx -1.2 \times 10^5$
12	55	40	-505	$\approx -2 \times 10^4$
13	45	10	-1195	$\approx -1.2 \times 10^4$
14	35	10	-525	$\approx -5.25 \times 10^3$
15	25	10	-1025	$\approx -1 \times 10^4$

There is excess heat in all of the different temperature intervals. This large availability in each of the temperature intervals indicated that the pinch temperature for this specific system was high. It was therefore decided that the network configuration would be designed below a pinch temperature of 1000°C.